ETHYLBENZENE DISPROPORTIONATION AND ETHYLATION OVER ZEOLITE BASED CATALYSTS: EFFECTS OF ZEOLITE STRUCTURE AND ACIDITY

BY

Mogahid Osman

A Thesis Presented to the
DEANSHIP OF GRADUATE STUDIES

KING FAHD UNIVERSITY OF PETROLEUM & MINERALS

DHAHRAN, SAUDI ARABIA

In Partial Fulfillment of the
Requirements for the Degree of

MASTER OF SCIENCE

In

CHEMICAL ENGINEERING

October 2013

KING FAHD UNIVERSITY OF PETROLEUM & MINERALS

DHAHRAN- 31261, SAUDI ARABIA

DEANSHIP OF GRADUATE STUDIES

This thesis, written by **Mogahid Osman** under the direction his thesis advisor and approved by his thesis committee, has been presented and accepted by the Dean of Graduate Studies, in partial fulfillment of the requirements for the degree of **MASTER OF SCIENCE IN CHEMICAL ENGINEERING.**

Mozahar Hossain

Dr. Mohammad M. Hossain
(Advisor)

Dr. Usamah A. Al-Mubaiyedh
Department Chairman

Dr. Sullaiman S. Al-Khattaf
(Co-Advisor)

Nadhir A. Al-Baghli

Dr. Salam A. Zummo
Dean of Graduate Studies

Dr. Nadhir Al-Baghli
(Member)

30/12/13

Date

Dr. Abdallah Al-Shammari
(Member)

Dr. Nabil Al-Yassir
(Member)

Dedication

To my parents who pick me whenever I fail, wipe my tears whenever I cry, Know my Fears and really care..

For everyone who taught me that nothing is out of reach..

To those who fill my moment with love and pleasure, my friends..

ACKNOWLEDGMENTS

My great thanks to Allah at first for giving me the strong will to continue and for sparing my life and guiding me to this point in my career.

I would like to acknowledge my indebtedness and gratitude to my advisor Dr. Mohammad M. Hossain for his guidance, unlimited support and encouragement throughout this study. Additionally, I am truly thankful to my Co-Advisor, Dr. Sullaiman S. Al-Khattaf, who in spite of his very tight schedule has found ample time to follow every step of this work making useful suggestions, corrections and directing the whole course of the work. My appreciation also goes to Dr. Nabil Al-Yassir for his efforts in the characterization and analysis of the catalysts used in this work. Also, thanks go to my other thesis committee members; Dr. Nadhir Al-Baghli and Dr. Abdallah Al-Shammari for their immense assistance throughout this work. Never would I forget also the contributions of Dr. Syed A. Ali particularly in the data analysis and Mr. Mariano Gica for always and patiently been around to assist in the experimental part of this work.

I would also like to thank the staff and postgraduates of the Chemical Engineering Department at KFUPM for their support throughout my study.

My sincere appreciation goes to my family who dedicates a lot of their precious time, assistance, and encouraged me to continue. Last but not least, I am grateful to all my friends for being the surrogate family during the many years of my stay in KFUPM.

TABLE OF CONTENTS

LIST OF TABLES

LIST OF FIGURES

NOMENCLTURE

C_i concentration of specie *i* in the riser simulator (mol/m^3)

CL confidence limit

E_i apparent activation energy of the *i*th reaction (kJ/mol)

k_i apparent rate constant for the *i*th reaction (m^3/kg of catalyst .s)

k_{oi} pre-exponential factor for the *i*th reaction after re-parameterization (m^3/kg of catalyst .s)

K_i adsorption constants for the *i* component

MW_i molecular weight of specie *i*

r_i rate of reaction for species *i*

R universal gas constant (kJ/kmol K)

t reaction time (s)

T reaction temperature (K)

T_o average temperature of the experiment

V volume of the riser (45 cm^3)

W_c mass of the catalyst (0.81 g)

W_{hc} total mass of the hydrocarbon injected the riser (0.162 g)

y_i mass fraction of i^{th} component

Greek Letters

α apparent deactivation function

λ catalyst deactivation constant (RC model)

η effectiveness factor

Abbreviations

BZ benzene

EB ethylbenzene

DEB diethylbenzene

TEB triethylbenzene

EtOH ethanol

ABSTRACT

Full Name : Mogahid Saifeldin Idris Osman

Thesis Title : Ethylbenzene disproportionation and ethylation over zeolite based catalysts: effects of zeolite structure and acidity

Major Field : Chemical Engineering

Date of Degree : October 2013

The disproportionation and ethylation of ethylbenzene has been studied over medium and large pore zeolite based catalysts in a fluidized-bed reactor. Focused is made on the effects of zeolites pore structure and acidity on activity, selectivity and reaction kinetics of EB disproportionation and ethylation. In this regard ZSM-5 with various Si/Al ratio and mordenite are selected as a medium and as large pore zeolites, respectively. The EB ethylation experiments are conducted using 1:1 EB to ethanol molar ratio and at various temperature levels and different contact times. The product analysis shows that diethylbenzene (DEB) is the main product. However, the large pore size mordenite catalyst also produces a small amount of triethylbenzene. Among the five HZSM-5 catalysts, the sample with SiO_2/Al_2O_3= 80 gives highest EB conversion and is more selective to DEB although the p-DEB/m-DEB for the catalysts are comparable with other samples. Phenomenological based kinetics models are developed based on the experimental conversion and selectivity data for EB ethylation. The Langmuir-Hinshelwood mechanism with surface reaction control is considered for both the medium and large pore zeolites. The analysis of the developed model suggests that a Langmuir-Hinshelwood mechanism with weakly adsorbed EB and strongly adsorbed ethanol and product DEB fits the experimental data adequately. The kinetic analysis also shows that the modenite requires significantly low activation energy (45.2 kJ/mol) as compared to the ZSM-5 zeolite (112 kJ/mol). On the contrary, the estimated enthalpy of adsorption of product DEB on mordenite (85.3 kJ/mol) is significantly higher than the value on the ZSM-5 sample (67.7 kJ/mol). The enthalpy of adsorption of ethanol is found to be 32.4 and 52.4 kJ/mole on mordenite and ZSM-5 samples, respectively. In EB ethylation, the HZSM-5 catalyst with SiO_2/Al_2O_3= 80 requires lowest amount of activation energy compare to other ZSM-5 samples; which is reflected in higher DEB selectivity of this catalyst.

ملخص الرسالة

الاسم الكامل: مجاهد سيف الدين إدريس عثمان

عنوان الرسالة: تفاعلات الإيثيل بنزين عن طريق ال (disproportionation) وال (ethylation) بإستخدام محفز الزيولايت: أثر بنية وحموضة الزيولايت.

التخصص: الهندسة الكيميائية

تاريخ الدرجة العلمية: أكتوبر 2013

يختص هذا البحث بدراسة تفاعلات الإيثيل بنزين عن طريق ال (disproportionation) وال (ethylation) بإستخدام الزيولايت المحفز متوسط وكبير المسام وذلك بإستخدام المفاعل المتطاير. تم التركيز على دراسة آثار مسام الزيولايت و الحموضية على النشاط والانتقائية وحركية تفاعلات ال (disproportionation) وال (ethylation). لهذا الشأن تم إستخدام المحفز (ZSM-5) ذو نسب مختلفة من السيليكات والألومينات (Si/Al) والمحفز (mordenite) حيث يمثلان محفزين بمسامية متوسطة واخر بمسامية كبيرة. تفاعل الكلة الإيثيل بنزين مع الإيثانول تمت بإستخدام موال واحد من الإيثيل بنزين مقابل كل مول من الإيثانول وفي ظروف مختلفة من درجات الحرارة والزمن. تحليل المنتجات أظهرت أن الدي إيثيل بنزين هو المنتج الرئيسي . ولكن إستخدام المحفز ذو المسامية الكبيرة أنتج أيضاً التراي إيثيل بنزين كمنتج جانبي. العينة التي تحوي نسبة سيليكات إلى الألومينات = 80 أظهرت أعلى نسبة تحويل للإيثيل بنزين كما أنها ذات إنتقائية عالية للداي إيثيل بنزين. تم تطوير نموذج مفصل لدراسة حركية التفاعل من خلال التجارب المنتقاة من المفاعل قيد الدراسة. تم إعتبار ميكانيكة التفاعل بإستخدام نموذج (Langmuir-Hinshelwood) مع فرضية حاكمية التفاعل السطحي لكل المحفزات المستخدمة في هذا الدراسة. من التحاليل والنموذج المطور أقترح نموذج (Langmuir-Hinshelwood) ليكون هو الأكثر ملائمة مع نتائج التجارب حيث تبين ضعف إمتصاص الإثيل بنزين و قوة إمتصاص الإيثانول والداي إثيل بنزين على سطح المحفزات. تحليل حركية التفاعل أظهرت أيضاً أن أظهرت أن قيمة طاقة التفاعل بإستخدام المحفز (mordenite) هي أقل مقارنة مع المحفز (ZSM-5). في المقابل قيمة إنثالبي الإمتصاص للداي إثيل بنزين على المحفز (mordenite) أكبر بكثير مقارنة مع القيمة المقدرة على المحفز ZSM-5)). إنثالبي الإمتصاص للإيثانول وجد يساوي (32.4 kJ/mole and 52.4) على المحفزات (mordenite) و (ZSM-5) بالترتيب. في تفاعل ألكلة

الإيثيل بنزين مع الإيثانول وجد أن المحفز الذي يحوي نسبة سيليكات إلى الألومينات = 80 يتطلب أقل طاقة تفاعل والتي إنعكست في الإنتقائية العالية للدي إيثيل بنزين بإستخدام هذا المحفز. وبالتالي المحفز الذي يحوي نسبة سيليكات إلى الألومينات = 80 يبدو أنه الأكثر كفائة لنشاطه وإنتقائيته الأعلى للداي إيثيل بنزين.

CHAPTER 1

INTRODUCTION

1.1. Background

Alkylation, transalkylation, isomerization, and disproportionation are important processes for the synthesis and the interconversion of alkylbenzenes. The chemical reactions involved in these processes are catalyzed by acids. During the past three decades, the main innovation in this field has been represented by the introduction of new zeolite catalysts with the aim to improve the overall selectivity of the processes and to comply with the requirements of the more stringent environmental legislation. Aromatics, together with light olefins, are the most important building blocks on which a vast petrochemical and organic chemical industry is based. They are important raw materials for many commodity petrochemicals and valuable fine chemicals such as monomers for polyesters, polyamides, and engineering plastics and intermediates for detergents, pharmaceuticals, agricultural products, and explosives [1].

Alkylation of aromatics, an important acidic catalytic reaction, has gained a tremendous interest in the petrochemical industry. High value common alkylaromatics products such as diethylbenzene, xylenes, cumene, cymene and isopropyltoluene are produced by catalytic alkylation of aromatics. Among these alkylaromatics para isomer of diethylbenzene (p-DEB) is an important starting material for chemical and petrochemical industries. It is commonly utilized as monomer for the production of ion

exchange resin and viscosity modifiers for lubricating oil [2]. A significant amount of the produced p-DEB goes in producing divinylbenzene (DVB), an intermediate used as a cross-linking agent in the manufacture of certain plastics [3]. p-DEB is employed as a desorbent in UOP para-ex and IFP-eluxyl desorption processes [2,4]. It also works as an additive in industrial heat transfer fluids. Accounting for all the after mentioned applications, there is a constant demand for the routine make-up requirements of existing operating units, with estimated consumption of 8000 tons/year. In addition, there are requirements for new loads of p-DEB for grass root units, with estimated demand of around 4000 tons/year. Therefore, the current worldwide demand for p-DEB is estimated to 12000 tons per years, which is expected to grow further [3]. With the present market prices of $4000/per metric ton, the annual sales volume is approximately around US$ 48 million dollars [3]. Considering the attractive price and increasing demand, in recent years there are significant initiatives to increase the p-DEB productions.

1.2. Diethylbenzene production

Conventionally, p-DEB is produced by reduction of diacetophenone. The other alternative routes are, disproportionation of ethylbenzene (EB) and/or alkylation of EB with ethanol, ethylene, or ethyl chloride [2, 4, 6] according to the following reactions:

Disproportionation of ethylbenzene:

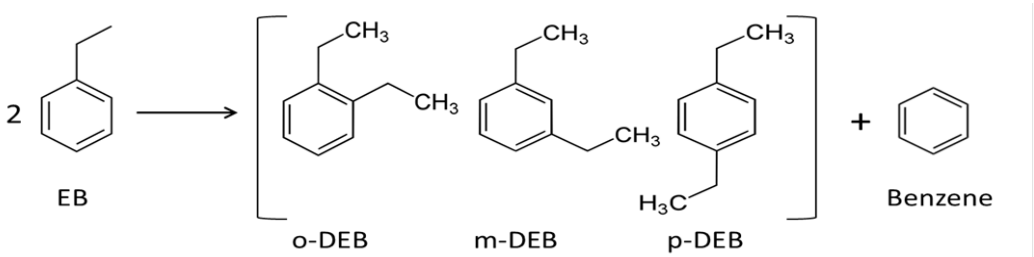

Alkylation of ethylbenzene with ethanol:

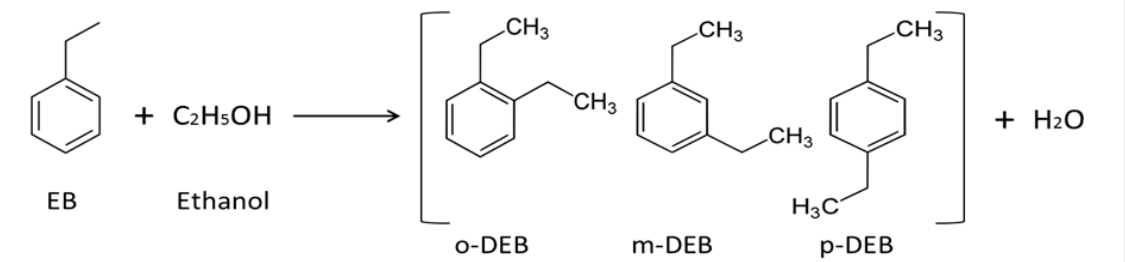

One can see from the above alternative routes; alkylation of each mole of EB gives one mole of DEB while the disproportionation of EB requires two moles of EB to produce one mole of DEB. Also, disproportionation gives one mole of benzene per mole of DEB produced. Therefore, the alkylation with an appropriate agent appears to be more preferable. Among the after mentioned alkylation agents, ethanol is considered to be the most economical due to its ample availability and relatively cheaper prices. From the technical view point, ethanol is also desirable given that the water produced during

alkylation with ethanol helps suppressing the coke formation, resulting sustained catalyst activity for longer period of time. To apprehend the advantages of EB alkylation with ethanol there are significant research initiatives have been under taken around the world to develop industrial scale EB alkylation technology.

A schematic flow diagram depicted in Fig. 1.1 for p-DEB selectivation process using modified ZSM-5 by Si-CVD surface silylation method was successfully commercialized by TSMC (Taiwan Styrene Monomer) in 1988. The commercial plant that produced p-DEB with 96% purity began its operation in 1990 with an annual production capacity of ca. 4000 tons/year. Recently, TSMC further upgraded their p-DEB production purity to 99%; representative analysis resulted into two commercial grade products. The TSMC process has a cycle length of over six months and its catalyst is fully regenerable [3].

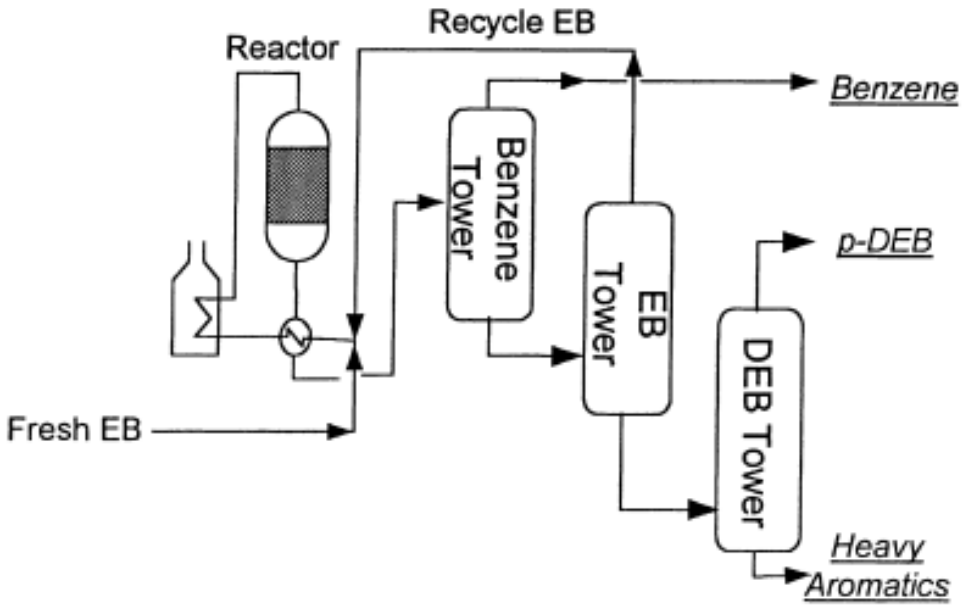

Figure. 1.1 Schematic flow diagram for p-DEB selectivation process

Recently, a few p-DEB processes utilizing the selective EB ethylation reaction scheme have also been developed. For example, Halgeri et al. [7] reported a new process that was developed by Indian Petrochemical, which utilized a modified ZSM-5 catalyst. The fully regenerable catalyst has a cycle length of over four months and the p-DEB purity increased with day-on-stream from 96% up to 99% at the end of cycle. The profile of the process is presented in Table 1.1.

Parameters	Range
Reactant	Ethylbenzene+ethylene
Reaction temperature	325–375°C
WHSV	1.5–2.0 h^{-1}
EB conversion per pass	10–12%
Cycle length	Over four months
p-DEB selectivity	96–99%

Table. 1.1 p-DEB manfucturing process by Indian Petrochemical [7]

1.3. Scope and objectives of the thesis

The main objectives of this work are explained in the following sections.

1.3.1 Initiation of a novel fluidized bed process for ethylbenzene ethylation and disproportionation

The main objective of this work is to initiate a fluidized bed process for ethylbenzene ethylation and disproportionation to produce diethylbenzene over fluidizable zeolite based catalysts using short reaction times. It is expected that the use of short contact times can restrict undesirable secondary reactions like further diethylbenzene ethylation and ethylbenzene cracking. In addition, it is believed that the use of short contact times as a means of increasing the yield of diethylbenzene and the proportion of para-diethylbenzene (measured by P/O and P/M ratios) in the reaction product can serve as a suitable alternative to repeated catalyst modification. Experiments will be carried out at different reaction conditions (temperature and time) to determine the effects of these reaction conditions on the following important variables

- Ethylbenzene conversion.
- Diethylbenzene yield.
- Triethylbenzene yield.
- P/O and P/M ratios.

1.3.2. Study the effect of SiO_2/Al_2O_3 ratio on ethylbenzene reactions

One of the main objectives of this study is to investigate the effects of acidity of HZSM-5 catalyst on the conversion of ethylbenzene and DEB selectivity for both the disproportionation and ethylbenzene alkylation with ethanol. In this regards, the HZSM-5 zeolites will be modified to various SiO_2/Al_2O_3 ratios (27, 55, 80, 150 and 280). ZSM-5 was chosen because of its remarkable shape selective properties which can be used to enhance the proportion of para-diethylbenzene in the reaction product.

1.3.3. Study the effect of zeolites pore structure on ethylbenzene reactions

The size of the zeolite channels plays a significant role in catalytic reactions. The pore size of the zeolite in combination with the sizes of the aromatic hydrocarbon and of the alkylating agent is the parameters that determine the alkylation activity and mechanism.

One of the goals of this study is to compare the behavior of a 10-ring pore member zeolite such as ZSM-5 (medium pore size) with that of a 12-ring pore member such as MOR zeolite (large pore size) on the activity, selectivity and mechanism of ethylbenzene ethylation reaction.

1.3.4 Kinetic modeling

Key to any process development is the availability of important design parameters such as the activation energy of the reaction, rate constants, etc.

Therefore kinetic modeling of ethylbenzene ethylation and disproportionation over all the catalysts used forms a major part of this work. The modeling will be carried out as follows:

I. Proposing different possible reaction models (power low model and phenomenological based model).

II. Fitting experimental data into the proposed models to check the validity of the models.

III. Determination of models parameters; apparent activation energy, adsorption enthalpies, apparent reaction rate constants and catalyst decay constants.

1.4. Thesis Outline

Chapter 2 gives a detailed review about the present issues in the literature concerning ethylbenzene alkylation and disproportionation reactions. General, mechanistic issues and kinetics of this reaction as well as current theories concerning the acidity of zeolites and its influence on catalysis are discussed.

Chapter 3 deals with the experimental section. Description of the equipment used for the experimental set-up is given as well as the procedures adopted. This chapter also explains the catalysts synthesis, characterization and evaluation.

Chapter 4 is dedicated to the experiments that were performed. The first part focuses on characterization of the catalysts used. Discussion of the effects of reaction conditions (temperature and time) are given in details. Effect of acidity and pore structure on ethylbenzene reactions also are given in detailed. In addition, a detail kinetic modeling of the reaction over all the catalysts is presented starting first with model formulation and then estimation of the kinetic parameters using non-linear regression analysis.

Chapter 5 gives the summary of our contribution and conclusions.

CHAPTER 2

LITERATURE REVIEW

2.1. Background

It was discussed in Chapter 1 that the favorable route for the production of DEB is based on ethylbenzene alkylation with ethanol forming DEB in the presence of an acidic catalyst, such as zeolites, under moderate reaction conditions.

The first step of the DEB production is the reaction between ethylbenzene and ethanol forming DEB (Fig. 2.1a) and the DEB could further react with ethanol forming TEBs (Fig. 2.1b). The later reactions are known as polyalkylation and the products of these reactions are polyethylbenzenes. Subsequently, the transalkylation of polyethylbenzenes could take place until the thermodynamic equilibrium is reached (Fig. 2.1d and e). These typical acid catalyzed ethylbenzene alkylation reactions are followed by a number of side reactions. The cracking of ethylbenzene and DEB and the oligomerisation of light alkenes which is leads to the formation of larger alkenes and these very reactive large alkenes could crack into smaller alkenes.

2.2. Catalysts for ethylbenzene transformation

The most widely used catalysts for ethylbenzene transformation reaction at present are based on zeolites; a special class of microporous crystalline solids which occurs naturally as minerals. Zeolites are also synthesized on a commercial scale for applications like adsorption separation, purification of commercial waste water

containing heavy metals, and nuclear effluents containing radioactive isotopes. The following sections give a brief insight into the different forms of zeolites and their applications in ethylbenzene transformation.

2.2.1. Zeolites

Zeolites become one of the most important catalysts in hydrocarbon reactions over the past 50 years due to their shape selective and environmentally friendly properties. They are well-defined microporous crystalline naturally occurring aluminosilicate minerals with a three-dimensional framework built up by SiO_4 and AlO_4 tetrahedra. These tetrahedrals are structured such that the oxygen at each tetrahedral corner is shared with an identical tetrahedron (Si or Al). The channels and cavities, which contain water molecules along with cations, are necessary to balance the charge of the framework [8, 9].

The general formula for a zeolite is:

$$M_{x/n}[(AlO_2)_x(SiO_2)_y] \bullet zH_2O$$

where M is the non-framework metal ion, n is the valence of cation M, x and y are integers with $y/x \geq 1$, z is the number of water molecules in each unit cell [9].

Zeolites are widely involved in conventional chemical reactions because of their unique properties. Zeolites are highly well structured, which give high products selectivity, and are extremely thermally stable, that can be operated at moderate temperature (250 – 300^{o}C) [10, 11]. Zeolites are used as catalysts in various complex hydrocarbon transformations because their acid-base properties can be modified during their synthesis, or by post-synthesis treatments [11].They have great adaptability and can

function as carriers of redox components in well-dispersed form [11]. Highly-silica zeolites such as ZSM-5 are attractive catalysts form any industrial processes because of their shape selective, well-defined pore structure, hydrothermal and acidic stability, high activity, and temperature and coke resistance properties [12, 13, 14].

On the other hand, the well-defined pore structure of zeolites limits the size of synthesized molecules; hence the formation of large molecules via zeolite-based catalysts is not favorable. Moreover, zeolites are highly sensitive to the deactivation caused by coking. The access of the reactant to the active sites in zeolites can be blocked even by small amount of coke [11].

The performance of zeolites in the synthesis of hydrocarbons within the zeolite framework structures depends on the shape selectivity effects and the strong Brønsted acidity of bridging Si-(OH)-Al sites generated by the presence of aluminum inside the silicate framework [15, 16]. The shape selective properties of zeolite catalysts allow molecules with critical kinetic diameter lower than the channel diameter to enter the pores, to react on the acid sites or, to exit the channels, and to be recovered as the products of the reactions [15]. Zeolites with pores less than 2 nm are categorized as highly structured microporous inorganic solids [10]. The acid strength of the zeolite is strongly connected to the Brønsted acid sites, i.e. catalyst protonation ability and bridging hydroxyl groups. Many researchers have proved that the acid strength of the zeolite is inversely proportional to the aluminum (Al) content [12, 13, 14]. It was shown that each type of zeolites would approach the optimum acidity at a specific Al content [16].

On the other hand, 'real' zeolite catalysts are usually pre-treated in various ways and have imperfect crystalline structure, such as the extra-framework aluminum sites. The presences of these sites are common and they either act as active sites or as sites that hinder the molecular diffusion [15]. It is mentioned above, that the activity of the zeolite acid catalysts is strongly affected by the catalyst framework and the acid strength. Hence, the characterization of zeolite catalysts has been mainly focused on the chemical properties, such as catalyst acidity, and the physical properties, such as pore size of the zeolites.

ZSM-5 zeolite is widely applied in industrial scale production of alkylbenzene, xylene and toluene [17]. ZSM-5 is medium-pore, 10-membered rings zeolite [17]. Figure 2.1 shows the pore structure of ZSM-5. The pore structure of ZSM-5 consists of one vertical channel with elliptical shape (5.1Å × 5.6Å) interconnected with another, sinusoidal near-circular channel (5.4Å × 5.6Å) [9, 10].

These pore structures form the unique shape-selective properties of ZSM-5. For example, the pores of ZSM-5 are extremely efficient and selective to the diffusion and desorption of para-diethylbenzene with respect to other isomers [17].

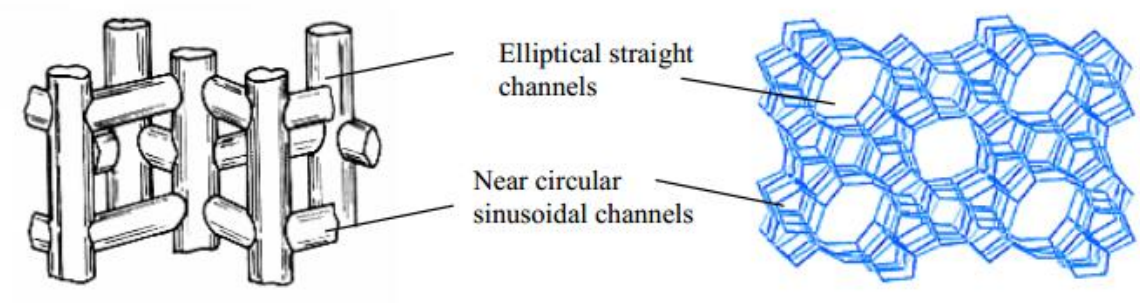

Figure 2.1. The channels and framework of ZSM-5 zeolite [17].

The activity of zeolites is determined by the presence of Brønsted acid sites, which originate from the creation of hydroxyls within the zeolite pore structure. Hydroxyls are formed by ammonium or polyvalent cation exchange or direct exchange with mineral acid for high-silica zeolites [11]. Hydroxyls are protons associated with negatively charged framework oxygens associated with alumina tetrahedral, as shown in Figure 2.2 below.

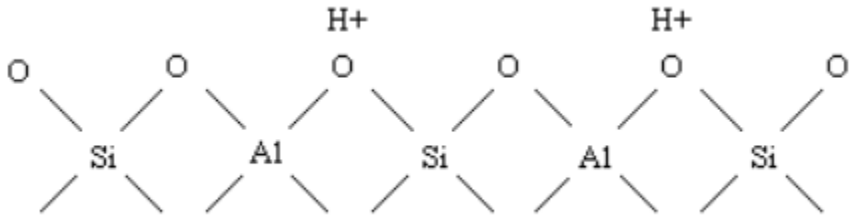

Figure 2.2. Bronsted acid sites in zeolites.

Dyer [9] illustrated that great mobility of protons are observed when the temperatures exceeded 200^{o}C and at 550^{o}C these protons are lost as water forming Lewis acid sites. Figure 2.3. illustrates this step.

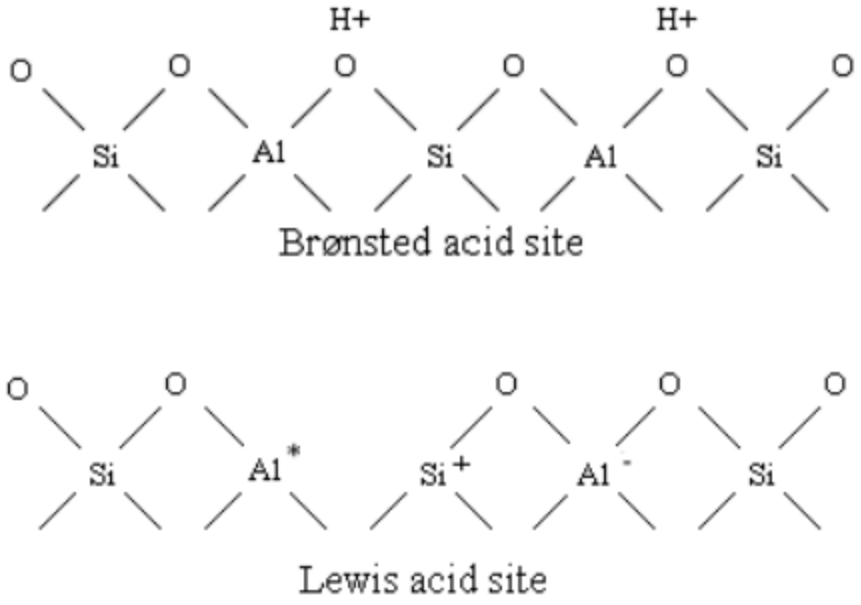

Figure 2.3. Conversion of Bronsted acid sites to Lewis acid sites.

The catalytic active sites exist in the pores, on the external surface and at the pore mouth of the zeolite crystals. The active sites in the pores are responsible for the formation of desired reaction products, while, the sites on the external surface and at the pore mouth may favour the formation of the unwanted non-selective catalysis. The unwanted non-selective reactivity could be avoided by limiting the external surface and the extra-framework material, by producing large well crystallized zeolite crystals [15].

2.2.2 Structure/Types of zeolites

Depending on the connections between the individual tetrahedra, channels of microporous dimensions up to 1.0 nm and /or cavities can be formed. The diameter of the channel window is governed by the number of tetrahedra forming these windows. In the case of aluminosilicate molecular sieves, zeolites with windows consisting of 6, 7, 8, 9, 10, 12 and 14 member rings have been synthesized and described. It is evident that the size and shape of these windows control the sieving effect of the zeolites that has consequences for their adsorption and catalytic performance. Zeolites possessing windows with odd-membered rings are divided into the following groups:

1) Medium-pore zeolites (10-membered rings up to 0.55 nm) e.g., ZSM-5, ZSM-11, ZSM-35, MCM-22 (possessing 12-member ring pockets on the crystal surface) and TNU-9. TNU-9 represents new 3D zeolites with 10-ring channels systems, being rather similar to industrially the most frequently employed ZSM-5. The size of the channels of TNU-9 is 0.52 x 0.60 and 0.51 x 0.55nm, thus, a slightly higher compared with ZSM-5.

2) Large-pore zeolites (12-membered rings up to 0.75nm) e.g., zeolite X, Y, beta, mordenite, ZSM-12 and SSZ-33. Zeolite SSZ-33 (CON topology) possesses a channel system complied of intersecting 12-MR (member ring) and 10-MR pores; it is the first synthetic zeolite having 4-4 = 1 SBU (secondary building unit) in the structure [18].

3) Extra-large-pore zeolites (14-membered rings with pore diameter smaller than 1.0 nm); only two zeolites (CIT-5 and UTD-1) with 14-membered rings are known [19].

The most utilized structural types of zeolites for catalyzing aromatic reactions are shown in Figure. 2.4.

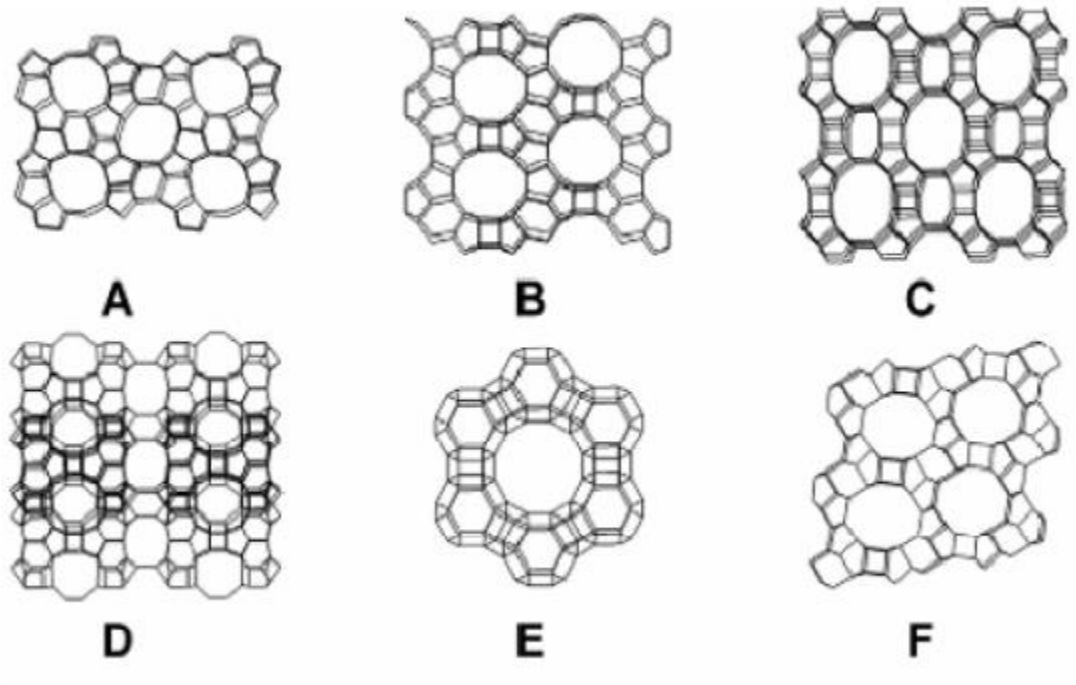

Figure 2.4. Structure of zeolites. ZSM-5 (A), mordenite (B), Beta (C), MCM-22 (D), zeolite Y (E), and zeolite L (F). (Taken from reference [19])

2.2.3 Advantages of zeolites over other solid acids as catalysts for aromatic transformations

The main advantages of zeolite and zeotype catalysts compared to conventional solid acids include.

1) Well-defined inorganic crystalline structures usually based on aluminosilicate (or metallosilicate) and aluminophosphate matrices, with a variety of structures differing in channels diameters, geometry, and dimensionality.

2) A precisely defined inner void volume providing high surface area up to 1200 m^2/g for mesoporous molecular sieves.

3) The ability to absorb and transform molecules in the inner volume.

4) Isomorphism substitution of some trivalent cations into the silicate framework enabling tuning of the strength and concentration of the acid sites.

5) Shape selectivity, given by the ratio of the kinetic diameters of the reactants, intermediates, and products to the dimensions of the channels.

6) Environmental tolerance.

2.2.4. Zeolite pore size and shape effects

The influence of pore size and shape on a reaction can be understood in terms of shape selectivity and confinement. Shape selectivity can be divided into three, well-accepted types:

1. Reactant shape selectivity: some reactants of the feed will fit into the zeolite pores and will react; others, which are too large, will not.
2. Transition state shape selectivity: when a transition state between a certain reactant and product is too large to be formed inside the pores, the corresponding product will not be detected.
3. Product shape selectivity: when a product is too large to exit the pores once it is formed, this product will also not be found.

2.3. Use of zeolites in ethylbenzene ethylation and disproportionation

Conventionally aromatic alkylation is carried out over Friedel Crafts catalysts. However, these types of catalysts have many technological and environmental impacts due to their corrosive nature and difficulty in separation, recycling and disposal.[7] Therefore, the current trend is to replace these catalysts by zeolites base catalyst, which are less corrosive and show high activity and unique combination of stability and shape selectivity in catalytic reactions. In the literature several types of zeolite base catalysts such as mordenite, USY, Beta, MCM-22 and ZSM-5 have been reported for the alkylation of ethylbenzene to produce p-DEB [20, 21]. According to these studies the acidity and pore structure are the two important parameters of the catalyst that influence the activity and product selectivity.

The main limitations of these catalysts is the low selectivity of p-DEB due to the thermodynamic equilibrium with other DEB isomers (para:meta:ortho = 30:54:16) [2, 22]. Cracking of EB on the acidic sites is the other important issue related to the zeolite base catalysts. It is not only consumes the EB feed to produce undesired products (mainly benzene) but also responsible for catalyst deactivation by coke formation.

Modification of the catalyst is one of the most widely accepted ways to increase the selectivity of p-DEB. There are two possible alternatives of modifying the zeolite based catalysts:

1) Passivation of the external acidic sites, minimizing the secondary isomerization of p-DEB (to form the m- or o-DEB) and cracking reaction and
2) Modifying the structure of the zeolite to facilitate the distinguishing diffusivities among p-DEB, m-DEB and o-DEB. [22-25].

The main challenge in the area of catalyst development for ethylbenzene ethylation and disproportionation is the development of a catalyst which can:

1) Produce high para-diethylbenzene selectivity while maintaining reasonable levels of ethylbenzene conversion.
2) Limit the major co-reactions like ethylbenzene cracking, diethylbenzene cracking and ethanol decomposition which occur simultaneously with the main alkylation reaction.
3) Resist quick deactivation.

Generally these may be achieved by modifying the physiochemical properties of zeolite catalysts. The properties which are usually modified include the overall acidity of the zeolite, the number of the external acid sites on the zeolite crystal, pore size and crystal size. Na, Fe, Mn, Al, La_2O_3 and CeO_2 are commonly used agents/metals to modify the zeolites for EB alkylation [25, 26]. Nitridation of parent HZSM-5 zeolites with flowing pure ammonia at high temperature can suppress the isomerization of para-DEB and leading to enhancement of para selectivity due to the absence of strong acid sites [24]. There are several studies reported the disproportionation and alkylation of EB on different HZSM-5 catalysts, most of them deals with effects of conversion of EB and p-DEB selective with various modified forms of HZSM-5. No attention has been paid to systematic evaluation of HZSM-5 with various Si/Al ratios. Regarding the structure modification, there are several alternatives controlling the pore sizes/structures of the zeolites [27]. Pre-coking is usually helpful of adjusting the pore opening size to increase the p-DEB selectivity [28]. However, studies show in addition to the positive impacts on the catalysts, both the passivation and shape adjustments may affect the active sites in

zeolite channels [27]. Therefore, both these techniques remain interesting topics for researchers to develop a highly active and p-DEB selective catalyst. Further, the Si-CVD surface treatment is an acid catalysis reaction during which the rate of deposition depends strongly on the acidity of zeolites. The external acidity can be eliminated without significantly changing the internal acidity by Si-CVD technique [29, 30].

In addition to ZSM-5 zeolite, a variety of other zeolites including mordenite and MCM-22 have been studied for the disproportionation and ethylation of ethylbenzene. Carrying out ethylbenzene disproportionation over MCM-22 and its dealuminated form at low temperatures, show that among the diethylbenzene isomers, *p*-DEB form within the micropore as the primary product. The *m*-DEB and *o*-DEB mainly produced via the secondary isomerization of the *para*-isomer on the external surface of the MCM-22 catalyst. And the *para* -selectivity increase with the degree of de-alumination, because this treatment preferentially removes the Brőnsted acid sites on the external surface that are responsible for the further isomerization of the *para*-isomer, rather than the acid sites within the micro-pores [5]. The removal of Al from the framework of mordenites essentially increases the catalytic activity and improves significantly the time-on-stream behavior of mordenite in the disproportionation of ethylbenzene. The formation of very strong acid sites caused by an increasing contribution from isolated (0-NNN) Al atoms in the framework seems to be the reason for the enhanced catalytic activity of de-aluminated mordenites. The changes in the micro-porosity created by de-alumination considerably improve the stability of the catalytic activity [26].

In addition to catalyst modification the contact time between the catalyst and the reactant/product also have significant influence on the selectivity of p-DEB. Short contact time fluidized bed reactors are favorable to improve the p-DEB selectivity using ZSM-based catalysts [2, 4, 31]. In fact, the alkylation of EB in fluidized bed offers three important advantages over the fixed bed operations:

i. Short contact time to minimize the further isomerization of p-DEB and reduces cracking reactions maximizing the p-DEB selectivity.
ii. Proper temperature control on the catalyst particles.
iii. Continuous catalyst regeneration.

2.3.1. Modification of external surface acid sites

As the selective synthesis and transformation of alkyl aromatics take place on acid sites located inside the zeolite channels, minimization or annihilation of the acid sites on the crystal surface, where the reaction environment is not limited by the steric constraints, is demanding. This can be achieved in two ways. By increasing crystal size of the zeolite, the relative concentration of acid sites inside the channels is increased compared to that on the crystal surface. However, due to the diffusional hindrance for alkyl aromatics inside the channels, the use of large crystals (ca > 2μm) leads to a substantial decrease in conversion values [19].

Another way of reduction of surface acid sites involves silylation of the crystal surface. This can be achieved by using the silylation reaction, which can take place either in solution or by the chemical vapor deposition (CVD) of chlorosilanes or alkoxysilanes [19]. To silylate exclusively the surface sites of ZSM-5 zeolite, tetraethyl- or isopropyl-

orthosilicates can be advantageously used, i.e., molecules whose kinetic diameters do not allow them to enter into the ZSM-5 zeolite pores, and the silylation reaction proceeds only with the protonic sites on the crystal surface.

2.4. Effect of Zeolite pore structure on ethylbenzene ethylation

In open literature there are several studies reported the alkylation of EB on different zeolite based catalysts dealing with effects of conversion of EB and product selectivity with various modified forms of zeolites. Surprisingly very less attention has been paid to study the effects of the zeolites pore size on the performance ethylbenzene ethylation reaction. The size of the zeolite channels plays a significant role in catalytic reactions. Generally, zeolites can be classified according to the pore size openings consisting of 8-, 10-, or 12- membered rings. Also, the pore system can be one, two or three dimensional, which contain pores of different sizes, and consist of tubes and/or cages.[32] The fact that the size of the channels is the same as the kinetic diameters of many organic reactants and products is the characteristic feature that forms the basis of the catalytic shape-selective behavior of zeolites [32]. In many aromatic alkylation, para selectivity was found to be higher over medium pore zeolites compare to large pore zeolites, medium pore zeolites have a channels with dimensions of about 0.55 nm which led to shape selectivity in the aromatic alkylation [33]. Moreover, large pore zeolite allows the formation of bulky products; while medium pore zeolite restricts the formation of the large molecules [34]. Arsenova et al. [35] found that medium pore zeolite H-ZSM-5 showed higher reactivity in the dealkylation of ethylbenzene due to its narrow channels and stronger Brønsted acid sites. Moreover, it has been demonstrated that ethylbenzene transformation reaction shows an induction period on large-pore zeolites and no induction period on medium-pore zeolites [35, 36].

2.5. Reaction mechanism and kinetic modeling

In ethylbenzene alkylation with ethanol over zeolite catalyst, DEB is initially formed in the primary step and the DEB formed could be converted further by secondary reaction steps. The EB reacts with ethyl carbenium ions via polyalkylation reactions, forming DEBs and TEBs (Eq. 2.1 and 2.2) [37].

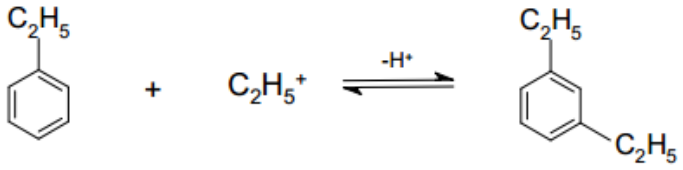

2.1

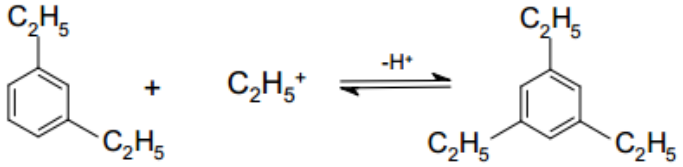

2.2

Ethylbenzene could be transformed via other side reactions include: the isomerization of EB into xylene isomers (Fig 2.5a); the dealkylation of EB forming benzene and ethylene (Fig 2.5b); the transalkylation of EB and xylene forming ethyltoluene and toluene, or dimethylethylbenzene and benzene (Fig 2.5c); the hydrogenolysis of EB producing toluene and methane (Fig 2.5d); and the disproportionation of EB which leads to the formation of benzene and DEBs (Fig 2.5e) [38]. Caeiro et al. [39] highlighted that ethylbenzene alkylation is thermodynamically limited and the dealkylation reaction (reverse step) contributes to the high alkane conversion, by forming significant amount of alkene that can be eventually transformed into aromatics.

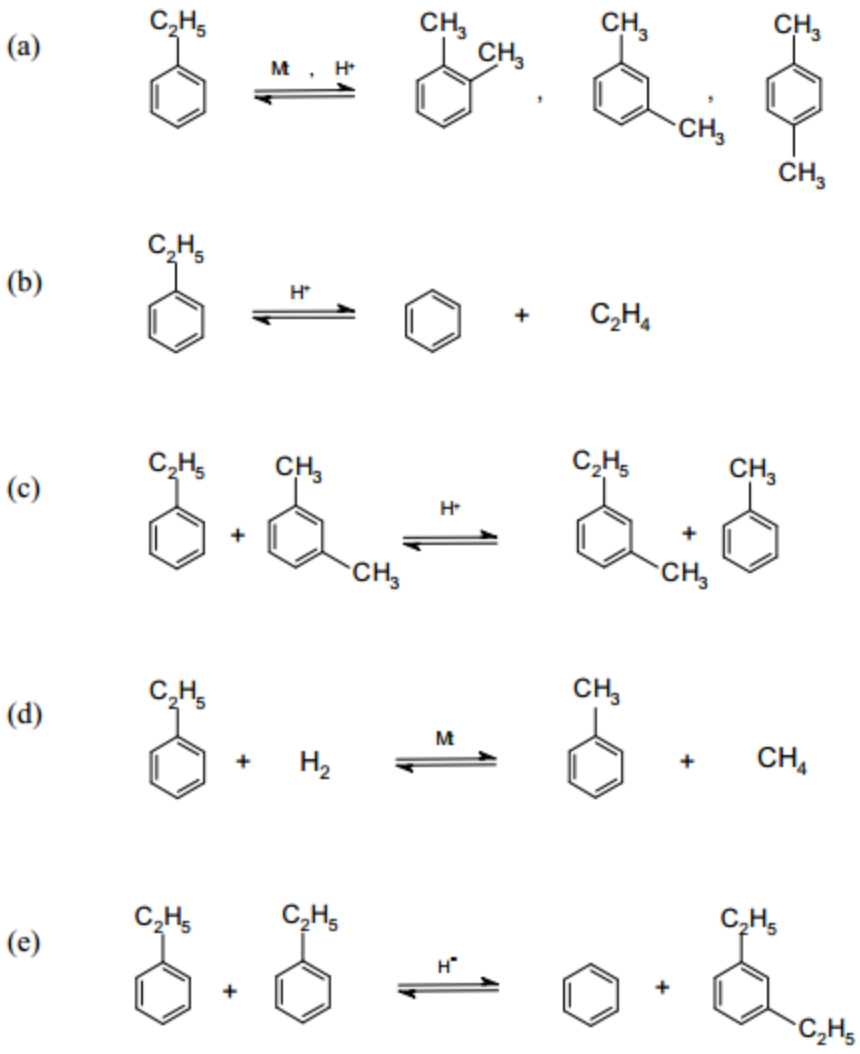

Figure 2.5. Main reactions of ethylbenzene over zeolite catalysts: (a) isomerization, (b) dealkylation, (c) transalkylation, (d) hydrogenolysis, (e) disproportionation (Taken from Moreau et al. 2002)

Ivanova et al. [40] suggested that the disproportionation and the transalkylation steps occur simultaneously. Three mechanisms are proposed in the literature for the transalkylation and disproportionation of alkylbenzenes. One of the proposed mechanisms is the direct shifting of the alkyl group from one aromatic ring to another without intermediate formation of an alkyl carbenium ion. The second proposed mechanism involves the formation of alkyl carbeniumions as intermediates. In the

monomolecular mechanism, the alkyl group on the alkylbenzene undergoes C-C bond cleavage on acid site forming alkyl carbenium ion and benzene. The alkyl carbenium ion formed in the primary step alkylates another alkylbenzene producing dialkylbenzene (Fig. 2.6a). The third suggested mechanism involves bimolecular intermediates, where the aromatics rings are bridged by a carbon atom from the alkyl group. The bimolecular intermediates would eventually dissociate into dialkylbenzene and benzene (Fig. 2.6b) [40, 41, 42]. Santilli [40] highlighted that if the alkyl group of the reactant is small, the bimolecular mechanism would appear to be the lower energy process due to resonance stabilization of the carbonium ion intermediate. However, the carbonium ion intermediate is large and therefore, its formation may be hindered in catalysts with small pore size, such as ZSM-5.

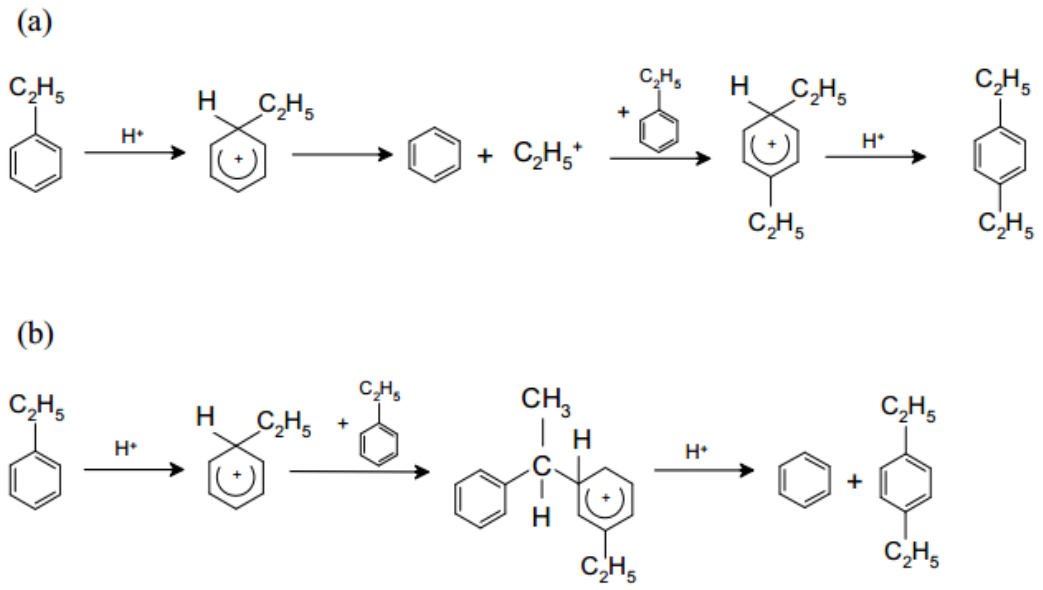

Figure 2.6. Disproportionation and transalkylation reactions of ethylbenzene: (a) molecular mechanism, (b) bimolecular mechanism [40, 41, 42]

Kinetic investigation of ethylbenzene disproportionation over large pore zeolites at low reaction temperatures evidenced that the reaction rate was strongly but reversibly retarded by the formation of the product DEB. In contrast, no product inhibition occurred over medium pore ZSM-5 [36]. In adsorption studies, *o*-DEB was shown to have restricted access to ZSM-5 channels. The first step considered in the ethylation of ethylbenzene is the formation of *p*-DEB inside the channels which isomerizes to a certain extent to the meta and ortho isomers on the external acid sites. In addition, crystal size was determined to have a very important role on the product distribution, with large crystals producing higher yields of *p*-DEB than those of smaller crystals [43]. Catalytic and sorption studies carried out by Arsonova-Hartel et al. suggest that the formation of o-DEB within the pores of ZSM-5 at low temperatures (less than 249 ^{o}C) is almost impossible. This suggests that o-DEB has restricted access to ZSM-5 channels. Recently, Pai et al. conducted a kinetic study of ethylbenzene disproportionation in a mixture of xylene over a modified HZSM-5 zeolite at temperatures of 573, 583, and 598 K. Based on a simple first-order model that was similar to that proposed by Nayak and Riekert, they were able to estimate the activation energy of the disproportionation reaction to be ~26.27 kJ/mol.

Regarding the kinetic model there are several models used to describe the catalytic alkylation of aromatics such as benzene ethylation, toluene methylation and benzene isopropylation. For example, the alkylation of toluene with isopropyl alcohol to form cymene has been described by a duel site Langmuir-Hinshelwood mechanism.[18] Sridevi et. al. [44] and Mantha et. el. [45] have also proposed a similar models for

ethylation of benzene and for methylation of toluene, respectively. In these model studies it was found that the large aromatic molecules have a tendency to interact strongly on the active sites compared to the smaller molecules. There are some studies unsuccessfully tried Eley-Rideal type model for alkylation of toluene with ethanol and ethylene over HZSM-5 [46, 47]. On the contrary, the alkylation of benzene with propylene over zeolites MCM-22 has been studied and the reaction mechanism proposed to follow Eley-Rideal approach in which benzene competes for the active site, but its coverage is much lower than that of propylene [48]. A kinetics study for the alkylation of benzene and toluene with methanol and ethylene over ZSM-5 (medium pore size) and Beta zeolite (large pore size) showed that the reaction mechanism follow Langmuir-Hinshelwood mechanism over ZSM-5 and Eley-Rideal mechanism over Beta zeolite [49]. However, in the open literature there are no research articles available reporting the phenomenological based kinetic model for the ethylbenzene ethylation reaction.

2.6. Thermodynamics of ethylbenzene reaction

The product distribution of DEB isomers in the reactions over ZSM-5 zeolites catalysts is affected by the thermodynamic equilibrium, geometrical restrictions as well as the diffusional limitation, i.e. the differences in the diffusivities of various product molecules [50]. Generally, the fraction of para-isomer is expected to be enhanced while the ortho isomer would be suppressed, since the formation of the smaller m/p-diethylbenzenes in the shape selective ZSM-5 zeolite catalyst is more favourable compared to the formation of bulkier o-diethylbenzene. The distribution of DEB isomers is also affected by thermodynamic equilibrium [51]. Table 2.2 shows the thermodynamic equilibrium of DEB isomers at different temperatures.

Table 2.1. Thermodynamic equilibrium of DEB isomers [51].

Temperature (^{0}C)	p-DEB (%)	m-DEB (%)	o-DEB (%)
100	33.2	54.7	12.1
200	31.3	53.7	15.0
300	29.8	52.7	17.5
400	28.5	52.0	19.5
500	27.5	51.3	21.2
600	26.7	50.7	22.6

Schumacher and Karge [50] pointed out that the diffusivity of para isomer in ZSM-5 zeolite catalyst is of the same magnitude as those reported for monosubstituted benzenes and benzene. Owing to the large differences of the transport velocities of isomers, the para isomer produced primarily inside the zeolite diffuses much faster to the

external surface than the other disubstituted isomers. As a result, the selectivity towards the para isomer will be generally enhanced compared to other disubstituted isomers produced in subsequent isomerisation reactions.

2.7. Important variables in ethylbenzene transformation

The efficiency of ethylbenzene ethylation process is a function of the following important variables:

2.7.1. Ethylbenzene conversion

This is the ratio of the amount of ethylbenzene transformed into products to the amount originally present in the feedstock. Ethylbenzene conversion is usually expressed in percentages and it is given mathematically as:

$$\text{Conversion of EB, } X_{EB} = \frac{\text{wt\% of ethylbenzene converted}}{\text{wt\% of ethylbenzene fed}} \times 100\%$$

2.7.2. Diethylbenzene selectivity

This is an indicator of how much of the converted ethylbenzene goes into diethylbenzene. It is also expressed in percentages. Mathematically diethylbenzene selectivity can be defined as:

$$\text{Selctivity of DEB, } S_{DEB} = \frac{\text{wt\% of DEB produced}}{\text{ethylbenzene conversion}} \times 100\%$$

2.7.3. Para-diethylbenzene selectivity

This indicates the relative proportion of para-diethylbenzene in the mixture of diethylbenzene (formed). Mathematically, para-diethylbenzene selectivity is defined as:

$$\text{p-DEB selectivity} = \frac{\text{wt\% p-DEB produced}}{\text{wt\% total-DEB produced}} \times 100\%$$

Para-diethylbenzene selectivity is also commonly measured by the following important ratios:

- P/O ratio: This is the ratio of the amount of para-diethylbenzene to ortho-diethylbenzene in the reaction product.
- P/M ratio: This is the ratio of the amount of para-diethylbenzene to meta-diethylbenzene in the reaction product.

2.8 Summery

The literatures reviewed clearly indicate that although several works have been conducted with regards to ethylbenzene transformation over zeolite-based catalysts. However, some aspects, such as the effect of alteration the acidity by different SiO_2/Al_2O_3 ratio of ZSM-5 and zeolites pore structure on the activity and product selectivity of EB transformation have received less attention. Moreover, all the previously reported kinetic studies on ethylbenzene disproportionation and ethylation reaction have been conducted using fixed-bed reactors, which are known to have some limitations of temperature and concentration gradients. Also there are no research articles in the literature reporting a phenomenological based kinetic model for the ethylbenzene ethylation reaction.

CHAPTER 3

EXPERIMENTAL SECTION

The experimental section describes the equipment in the experimental set up and the procedures adopted in carrying out this work. The major tasks carried out here include catalyst preparation, characterization and evaluation.

3.1. Experimental Set-up

Experimental runs for ethylbenzene alkylation and disproportionation process were carried out in a riser simulator reactor. The reactor was connected to a vacuum box through a four-port valve.

The products were removed from the riser simulator at the end of the pre-set reaction period. A time/actuator assembly linked to the feed injection system controlled the four-port valve. The vacuum system was connected to a manually operated six-port sampling valve. This sampling valve was connected on-line to the gas chromatograph.

Furthermore, the riser simulator reactor and the vacuum box were equipped with pressure transducers to monitor the pressure during and after the reaction periods. Both the reactor and the vacuum system were supplied by separated heating systems and both were well insulated. The feed injecting system includes a gas tight syringe connected to switches to control the timer/actuator assembly on the four port valve and the data acquisition system. The data acquisition system allowed monitoring the change of

pressure with time from both the reactor and the vacuum box. A four-port valve, controlled by a timer/actuator assembly, was linked to the injection system. A vacuum system was also connected to the manually operated six port sampling valve which allows for sampling injections into the gas chromatograph. Both, the reactor and the vacuum system are located in temperature controlled ovens. Connections between components are accomplished using heated and well insulated lines. The unit was also equipped with two pressure transducers which allowed for continuous pressure monitoring during the reaction and post-reaction evacuation periods. A schematic diagram of the experimental setup is given in Figure 3.1.

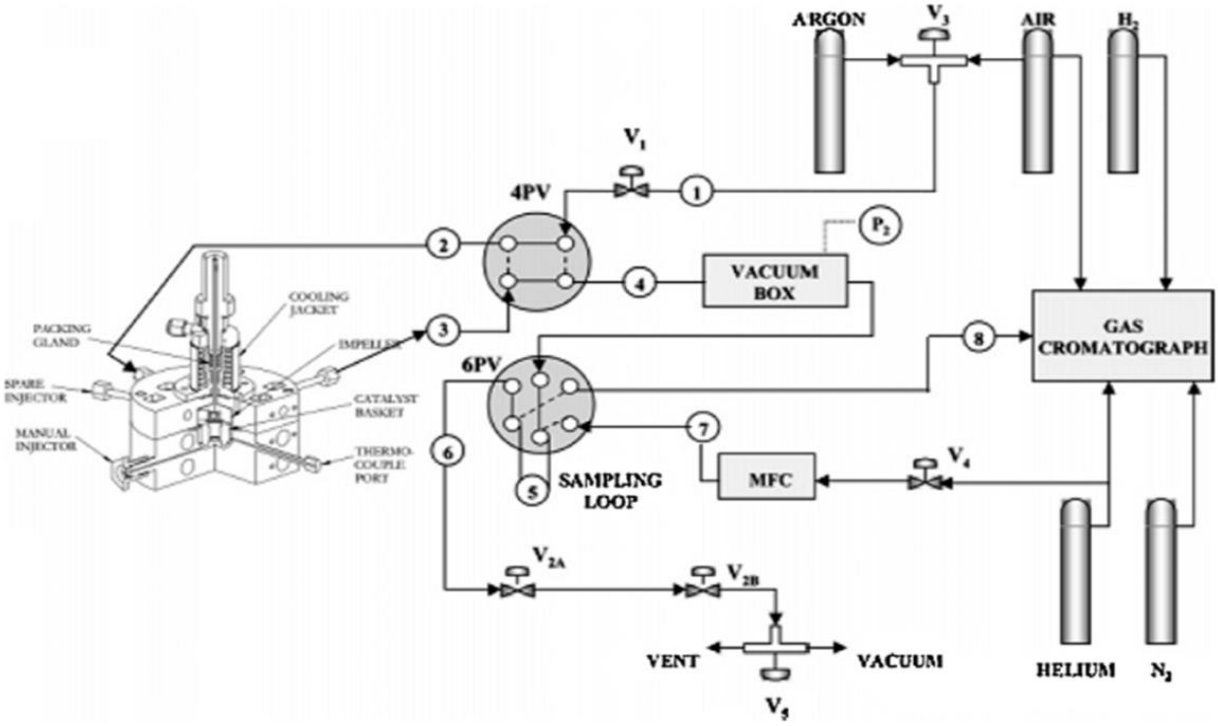

Figure 3.1. Schematic diagram of the riser simulator experimental set-up

3.1.1. Riser Simulator

This novel reactor was invented by de Lasa [52] and it was designed to provide high gas phase circulation rates as well as intense catalyst mixing. In this respect, perfect mixing with the absence of coke profiles and gas channeling can be obtained with all catalyst particles being exposed to the same reaction environment. As mentioned by Pruski et. al. [53], good fluidization is achieved under typical riser conditions and using shaft spinning rates close to 7600 rpm. The riser simulator can be used for several purposes: a) to test industrial catalysts at commercial conditions [54], b) to carry out kinetic and modeling studies for certain reactions, c) to develop adsorption studies [53], d) to use the data of this unit for assessing the enthalpy of cracking reactions. The riser simulator consists of two outer shells, the lower section and the upper section, which allow one to load or to unload the catalyst easily. The reactor was designed in such a way that an annular space is created between the outer portion of the basket and the inner part of the reactor shell. A metallic gasket seals the two chambers with an impeller located in the upper section. A packing gland assembly and a cooling jacket surrounding the shaft provide support for the impeller. Upon rotation of the shaft, gas is forced outward from the center of the impeller toward the walls. This creates a lower pressure in the center region of the impeller, thus inducing flow of gas upward through the catalyst chamber from the bottom of the reactor annular region where the pressure is slightly higher. The impeller provides a fluidized bed of catalyst particles as well as intense gas mixing inside the reactor. A schematic diagram of the riser simulator is shown in Figure 3.2

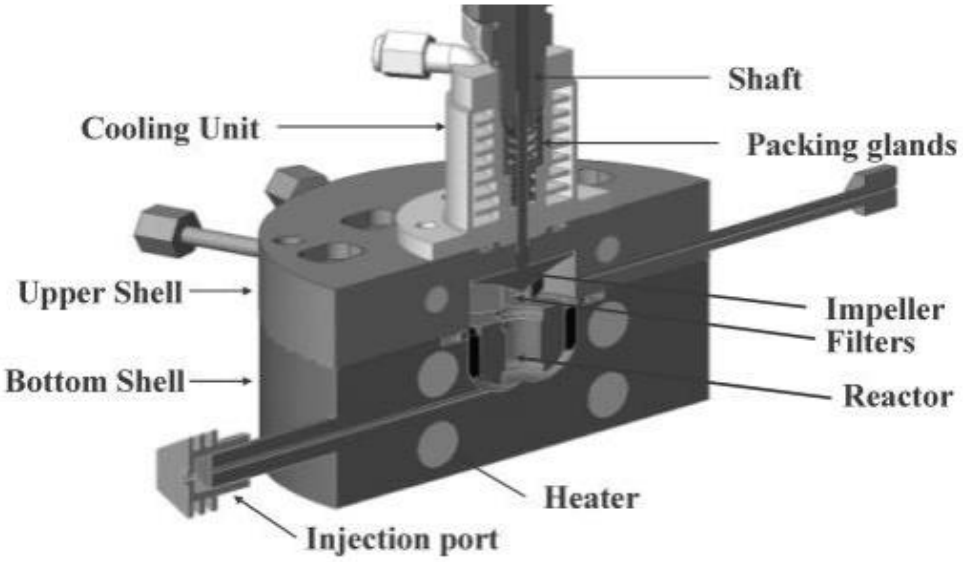

Figure 3.2a. Schematic diagram of the riser simulator

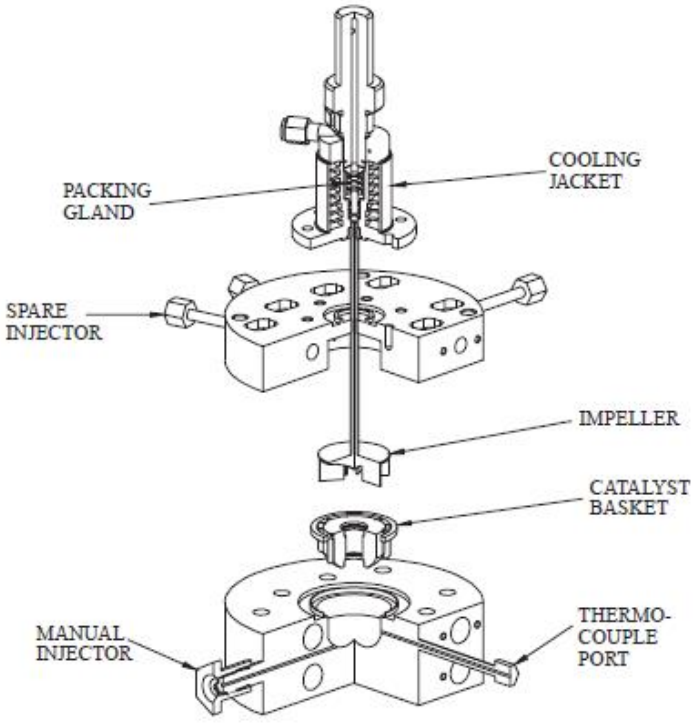

Figure 3.2b. Cross section of the riser simulator displaying the unit components

3.1.2. Gas Chromatograph (GC) System

The quantitative analysis of the reaction products were carried out online using an Agilent GC equipped with Flame Ionization Detector FID (Agilent Chromatograph Model 6890N), equipped with an HP-INNOWAX capillary column (Polyethylene glycol (PEG)) (length 60 m x internal diameter 0.32 mm x film thickness 0.50 mm). Helium is used as the carrier gas, while air and hydrogen gases are used for the FID detector.

Furthermore, liquid nitrogen is used to facilitate the initial cryogenic operation of the GC temperature program. The liquid nitrogen cools the GC oven to -30 °C. The flow of liquid nitrogen is administered by a solenoid valve actuated from the GC's internal oven temperature controller. The integrator allows strip chart recording as well as integration of the GC detector signal. The integrator is connected to the GC via a HPIL instrument network cabling system.

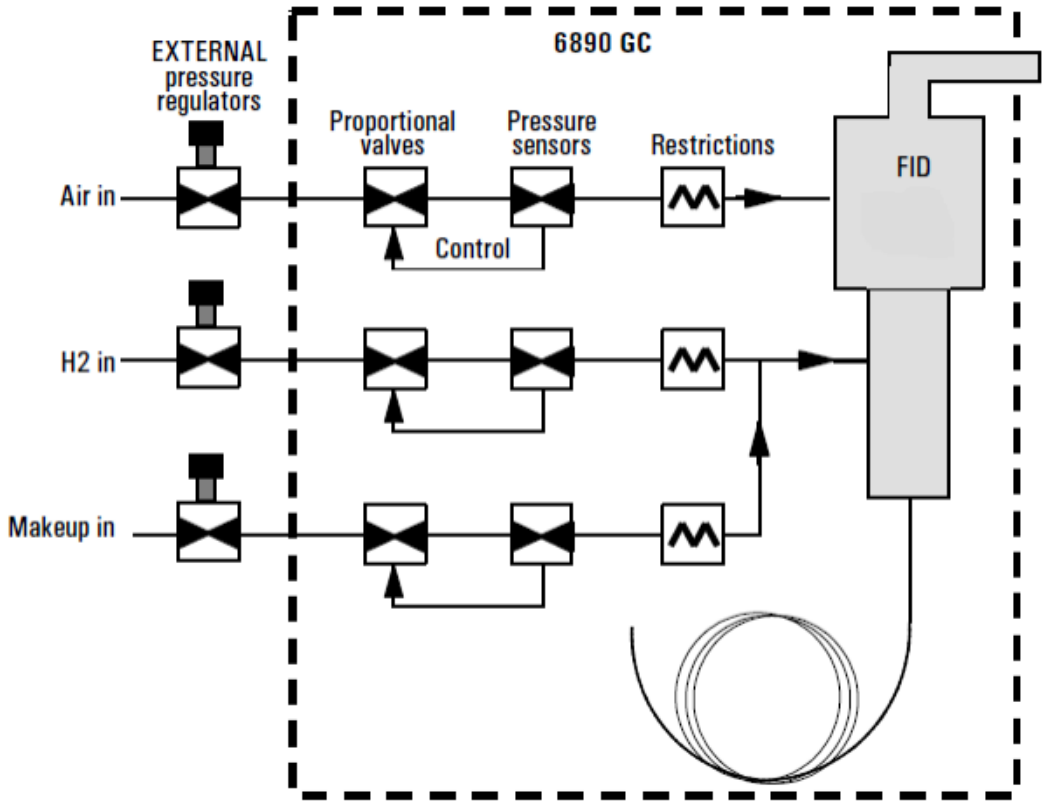

Figure 3.3. Schematic diagram of the gas chromatograph

3.2. Experimental procedure

3.2.1. Materials

The commercial zeolites used in this study was supplied by Zeolyst; ZSM-5 (CBV3024E, Nominal SiO_2/Al_2O_3 = 27, NH4-form; CBV5524G, Nominal SiO_2/Al_2O_3 = 55, NH4-form; CBV8014, Nominal SiO_2/Al_2O_3 = 80, NH4-form; and CBV28014, Nominal SiO_2/Al_2O_3 = 280, NH4-form). HZSM-5 of nominal SiO_2/Al_2O_3 = 150 (CT 412) was supplied by Catal. International Ltd. (UK). Prior to testing, the as-received NH4-form zeolites were calcined in standing air at 550 °C for 5 h (ramping rate of 3 °Cmin-1), in order to get the H-form. These zeolites are hereafter referred as HZ-27, HZ-55, HZ-80, HZ-150, and HZ-280, where the number represents the nominal SiO_2/Al_2O_3 ratio. Mordenite zeolite with silica to alumina ratio of 180 and 21 was obtained from Tosoh Chemicals, Japan. High purity grade of ethylbenzene and ethanol were obtained from Sigma-Aldrich.

3.2.2. Catalyst synthesis

All the Na-ZSM-5 and MOR samples were ion-exchanged with NH_4NO_3 to replace the Na^+ with NH_4^+. The samples were converted into the proton-exchanged form by calcination for 2 h at 600°C.

3.2.3. Catalyst characterization

Several techniques had been used for characterization of the catalyst samples used in this study include: X-ray power diffraction (XRD), BET surface area measurements to

understand the textural properties of the catalysts and FTIR Spectroscopy of pyridine adsorption to determine the types of available acid sites.

Atomic Absorbance: The chemical compositions were determined by atomic absorption spectroscopy, using the Perkin-Elmer equipment (Model AAS 1100B).

Brunauer-Emmett-Teller (BET) Surface area Measurements: The textural properties of all zeolite samples were characterized by N2 adsorption measurements at 77 K, using Quantachrome Autosorb 1-C adsorption analyzer. Samples were outgassed at 220 °C under vacuum (10-5 Torr) for 3 h before N2 physisorption. The BET specific surface areas were determined from the desorption data in the relative pressure (P/P0) range from 0.06-0.3, assuming a value of 0.164 nm 2 for the cross-section of the nitrogen molecule.

X-Ray Diffraction: The high-angle powder X-ray diffraction (XRD) patterns were recorded on a Shimadzu powder diffraction system using CuKα radiation (λKα1 = 1.54051Å, 45 Kv and 35 mA). The XRD patterns were recorded in the static scanning mode from 1.2 - 60° (2θ) at a detector angular speed of 0.01 °/s and step size of 0.02°.

NH_3-Temperature-Programmed Desorption: Temperature-programmed desorption of NH_3 (NH_3-TPD) was carried out using Quantachrome Autosorb 1-C/TCD equipped with a mass spectrometry detector (Cirrus 2, mks, spectra products). Samples were pretreated at 450 °C in a flow of helium (25 ml min^{-1}) for 2 h. This was followed by the adsorption of ammonia (5 vol.% in helium) at 100 ºC for 30 min. Samples were then purged in a He stream for 2 h at 120 ºC in order to remove loosely bound ammonia (i.e. physisorbed and H-bonded ammonia). Then, the samples were heated again from 100 to 700 ºC at a

heating rate of 10 ºC/min in a flow of helium (25 $mlmin^{-1}$) while monitoring the evolved ammonia using TCD.

FTIR Spectroscopy: Infrared spectroscopy of adsorbed pyridine was used to determine the types of available acid sites (i.e. Brönsted and/or Lewis acid sites). The measurements were carried out using a Fourier transform infrared using Nicolet FTIR spectrometer (Magna 500 model). The samples in the form of a self-supporting wafer (*ca.* 60 mg in weight and 20 mm in diameter) were obtained by compressing a uniform layer of powder. The wafer was then placed in an infrared vacuum cell equipped with KBr windows (Makuhari Rikagaku Garasu Inc., JAPAN), and pretreated under vacuum (*ca.* 10^{-3} Torr) at 450 °C for 2 h. The adsorption temperature of pyridine was 150 °C. For a quantitative characterization of acid sites, the following bands and absorption coefficients were used: pyridine (PyH^{+}) band at 1545 cm^{-1}, ε = 0.078 cm /μmol^{-1}; pyridine (PyL) bands at 1461 and 1454 cm^{-1}, ε = 0.165 cm/μmol^{-1} [2, 3].

3.3. Catalysts evaluation

The disproportionation and ethylation of ethylbenzene experiments were conducted using 0.80 g of catalysts with particle size of 60 µm. For the disproportionation reaction, pure ethylbenzene was as feed while 1:1 ethylbenzene to ethanol molar feed ratio was used as feed for the ethylation experiments. Before the actual runs, the catalyst was thermally activated at 620 °C for 15 min in the presence of Ar. Regarding the temperature variation, the experiments were performed at different temperature levels ranging between 200-400 ºC and atmospheric pressure before injection of the feed. After the injection, reactor pressure increased given the system is

operated in batch mode. The reaction time (contact time) was varied from 5 to 20 sec. After each run the product gas samples were analyzed three times by automatic injection into a GC. The standard deviations at each run were found in the range of ±2%. The GC analyzed data were further processed to calculate the conversion and selectivity using the following equations:

$$\text{Conversion of EB, } X_{EB} = \frac{\text{wt\% of ethylbenzene converted}}{\text{wt\% of ethylbenzene fed}} \times 100\%$$

$$\text{Selctivity of product i, } S_i = \frac{\text{wt\% of product i}}{\text{ethylbenzene conversion}} \times 100\%$$

$$\text{p-DEB selectivity} = \frac{\text{wt\% p-DEB produced}}{\text{wt\% total-DEB produced}} \times 100\%$$

CHAPTER 4

RESULTS AND DISCUSSIONS

This section presents and discusses the results of ethylbenzene ethylation and disproportionation over ZSM-5 and mordenite zeolite based catalyst. The effects of acidity and pore structure of the zeolite on the activity, selectivity and mechanism of EB reactions are discussed in details. The effect of reaction conditions (temperature and time) on important variables such as ethylbenzene conversion, diethylbenzene yield, the para-diethylbenzene selectivity are also discussed. In addition a detailed kinetic modeling of the reaction over all zeolite based catalyst carried out in this study is presented starting first with model formulation and then model parameters determination using non-linear regression analysis.

4.1. Effect of Si/Al ratio on ethylbenzene disproportionation and ethylation over ZSM-5 based catalyst:

4.1.1. Physicochemical properties of the catalysts

The specific surface area and pore volume determined by nitrogen physisorption for the HZSM-5 with different SiO_2/Al_2O_3 samples are listed in Table 4.1. The BET surface area of the samples compared well with the value given by the supplier. After ion-exchange, the surface area of all the samples significantly varied with the variation of the SiO_2/Al_2O_3 ratios. The specific surface area of HZSM-5 samples increased with the

increase of SiO_2/Al_2O_3 ratios (Table 4.1). The pore volumes of the samples are calculated to be 0.25, 0.25, 0.28, 0.26 and 0.23 for the SiO_2/Al_2O_3 ratio of 27, 55, 80, 150 and 280, respectively. Min and Hong [55] also reported similar behavior of HZSM-5 samples with SiO_2/Al_2O_3 varied between 21 and 36.

Table 4.1: Textural properties of MFI microporous aluminosilicate of different Si/Al ratios

Samples	SiO_2/Al_2O_3[a]	S_{BET} (m^2g^{-1})	S_{meso} (m^2g^{-1})	V_{micro} (cm^3/g)[b]	$V_{meso,N2}$ (cm^3/g)[c]
HZ-27	25.0	357	44.0	0.15	0.10
HZ-55	52.0	376	74.0	0.15	0.10
HZ-80	82.0	451	51.0	0.19	0.09
HZ-150	131.0	435	69.0	0.17	0.09
HZ-280	283.0	443	23.0	0.21	0.02

[a]: by Atomic Absorbance Spectroscopy (AAS); [b]: obtained from *t*–plot,
[c]: pore volume in the range of 4-100 nm derived from N_2 adsorption.

The XRD patterns of all the HZSM-5 zeolite samples with different SiO_2/Al_2O_3 indicate that the structure of the zeolite remained intact even with the significant variation of the SiO_2/Al_2O_3 ratios (Figure 4.1). Thus, the variation of the SiO_2/Al_2O_3 of the HZSM-5 zeolites affects only the acidity of the zeolite, without destroying the parent HZSM-5 structure.

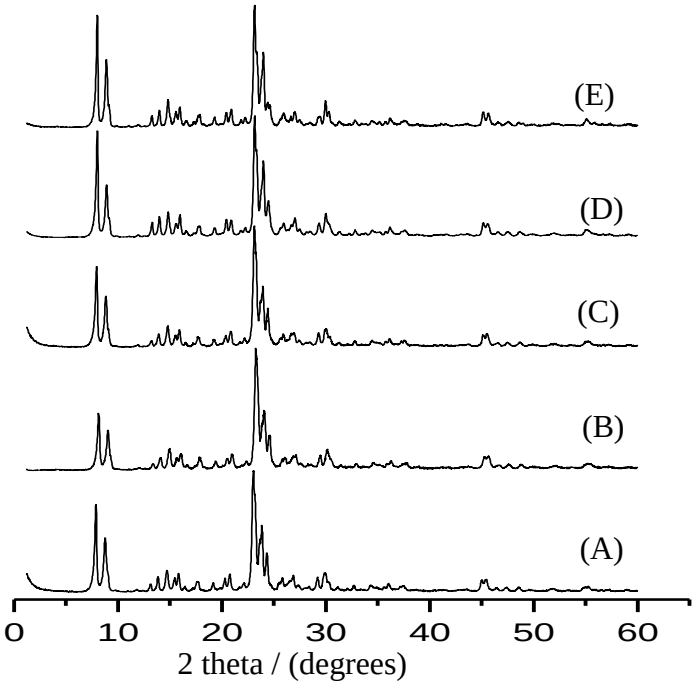

Figure 4.1 XRD patterns of MFI microporous aluminosilicate of different SiO_2/Al_2O_3; A) 27, B) 55, C) 80, D) 150, and E) 280.

The NH_3-TPD experiments shows that the HZSM-5 samples contain both low and high temperature peaks, corresponding to weak and strong acid sites, respectively (Figure 4.2a). The range of weak and medium strength acid sites were set at 200 – 300 °C, 300 – 450 °C, respectively. The acid sites appeared above 450 °C is considered as strong acid sites. Table 4.2 summarizes the amount and percentage of various types of acid sites. One can see in Table 4.2, with increasing SiO_2/Al_2O_3 ratios the total acidity of HZSM-5 samples decreased while the percentage of strong acidic sites (>450 °C) increased. The presence of Brönsted and Lewis acid sites were confirmed by the pyridine FTIR characterization (Figure 4.2b). The amount and percentages of each of Brönsted and Lewis type acid sites are also presented in Table 4.2. As it can be noticed that up to

SiO_2/Al_2O_3 = 80, the Brönsted acidic sites were decreased with increasing the SiO_2/Al_2O_3 ratio after that it started increasing slightly. On the other hand the Lewis acid sites were increased then decreased again with increasing the SiO_2/Al_2O_3 ratio. It is interesting to note that among the HZSM-5 samples, the sample with SiO_2/Al_2O_3 ratio of 80 shows a good balance between Brönsted and Lewis acid sites. An appropriate balance between the strong acidic sites with keeping the Brönsted acidic sites in the higher level is desirable for EB transformation reaction [56-58].

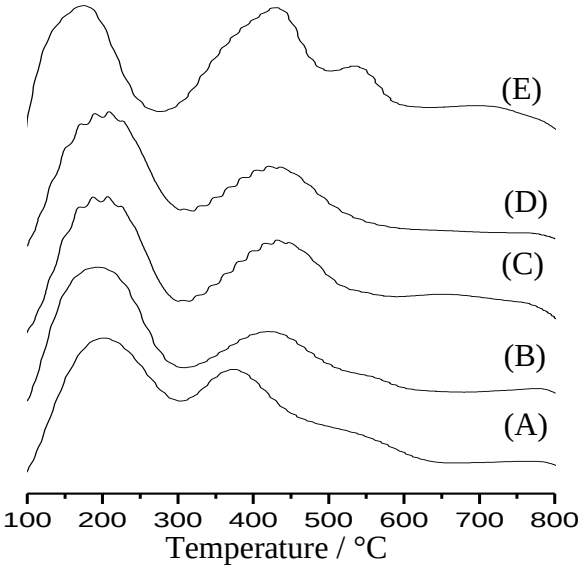

Figure 4.2a. NH_3 TPD profiles of MFI microporous aluminosilicate of different SiO_2/Al_2O_3; A) 27, B) 55, C) 80, D) 150, and E) 280.

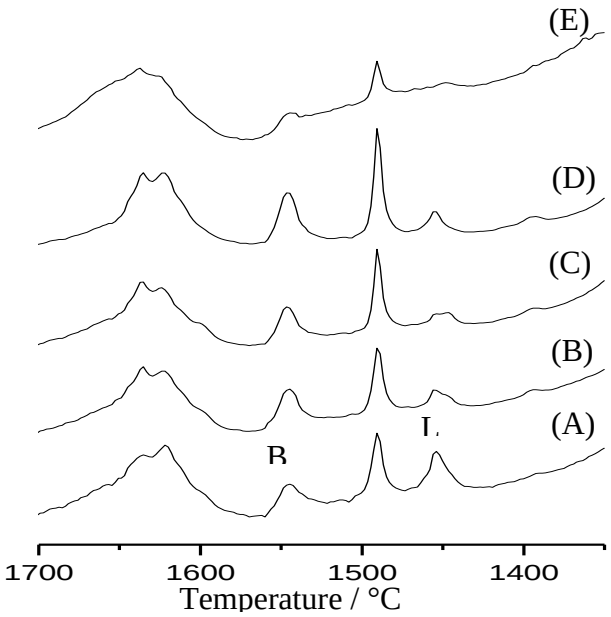

Figure 4.2b. FTIR of chemisorbed pyridine of MFI microporous aluminosilicate of different SiO_2/Al_2O_3; A) 27, B) 55, C) 80, D) 150, and E) 280 (B: Brönsted, L: Lewis acid sites)

Table 4.2: Acid sites characteristics of MFI microporous aluminosilicate of different Si/Al ratios

Zeolites	NH_3-TPD ($mmolg^{-1}$)[a]				FTIR-chemisorbed Pyr. ($mmolg^{-1}$)		
	T^b	L.T. (weak), 200 - 300 °C	H.T. (medium- strong), 300 - 450 °C [c]	460 – 575 °C [d]	T^b	B	L
HZ-27	0.730	0.484 (67%)[e]	0.226 (31%)	0.02 (2%)	0.751	0.650 (87 %)	0.101 (13 %)
HZ-55	0.458	0.261 (57%)	0.177 (39%)	0.02 (4 %)	0.300	0.290 (97 %)	0.01 (3 %)
HZ-80	0.354	0.194 (55%)	0.120 (34%)	0.04 (11%)	0.143	0.08 (56 %)	0.063 (44 %)
HZ-150	0.210	0.040 (19%)	0.120 (57%)	0.05 (24%)	0.130	0.079 (61 %)	0.051 (39 %)
HZ-280	0.094	0.025 (27%)	0.019 (20%)	0.05 (53%)	0.016	0.011 (69 %)	0.005 (31 %)

[a]: L.T. and H.T. correspond to low- and high-temperature NH_3 desorption peak, respectively; [b]: total number of acid sites, [c,d]: strong acid sites of Brönsted and Lewis nature, respectively; and [e]: number in parenthesis corrosponds to % of acid sites.

4.1.2. Disproportionation versus Ethylation of ethylbenzene

As mentioned in the experimental section, both the disproportionation and ethylation of EB experiments were conducted in a CREC Riser Simulator under fluidized bed conditions. In order to compare products compositions between disproportionation and ethylation, all the catalytic runs were carried out using same amount of EB feed. Table 4.3 presents the product analysis results of the disproportionation of EB over the HZSM-5 samples after 20 seconds of reaction at three levels of reaction temperatures (250, 300 and 350 °C). One can see that at all temperature levels diethylbenzene (DEB) and benzene were the main products. Among the DEB isomers p-DEB and m-DEB were dominant while a small amount of o-DEB was also detected under the present experimental conditions. The gaseous product predominantly ethylene but their overall composition is very low. The other hydrocarbon products such as triethylbenzene, toluene and gaseous hydro-carbons are negligible.

In disproportionation of EB the origin of benzene could be both disproportionation and cracking reactions [2, 4]. In this study at all temperature levels the HZSM-5 catalysts samples produced highest amount of benzene. This observation might lead one to speculate about the possibility of cracking especially for catalyst with high acidic site concentration. One way to confirm the occurrence of cracking is the product gas analysis which is also originated from the cracking reaction. As it can be seen in Table 3, the amount of product gas is minimal even at high EB conversion. This suggests that the benzene is mainly produced via the disproportionation reaction. Previously, the present research group demonstrated that higher reaction temperature (> 400 °C) favors the cracking reaction that produces undesired product benzene [4, 31]

using a USY catalyst. In the present study the catalytic runs were conducted well below 400 °C, as a result the cracking reaction is limited.

Table 4.3: Product distribution (wt%) of ethylbenzene disproportionation on HZSM-5 with different Si/Al ratio at 20 s reaction time.

Catalysts	Temp (°C)	EB conv. (%)	Product Yield (%)					
			Benzene	*p*-DEB	*m*-DEB	*o*-DEB	Total-DEB	Others[a]
HZ-27	200	7.07	4.42	1.18	1.44	0.07	2.69	-
	250	15.8	8.95	2.73	3.64	0.18	6.55	0.36
	300	41.01	22.2	3.73	6.44	0.46	10.6	4.18
	350	47.57	27.9	1.94	3.48	0.35	5.77	7.33
HZ-55	200	4.35	2.54	0.48	0.88	0	1.4	-
	250	14.7	7.3	2	3.93	0.17	6.1	-
	300	38.4	19.8	4.22	9.2	0.9	14.3	-
	350	48.5	27.35	2.66	5.75	0.77	9.2	-
HZ-80	200	2.40	1.73	0.28	0.36	0.00	0.64	-
	250	9.37	5.18	1.34	2.56	0.10	4	-
	300	27.53	13.04	4.13	8.40	0.90	13.43	0.35
	350	42.17	20.45	4.95	10.44	1.23	16.62	1.12
HZ-150	200	1.41	0.92	0.20	0.29	0.00	0.49	-
	250	5.83	3.11	0.92	1.65	0.0	2.57	-
	300	26.06	12.3	4.03	7.92	0.53	12.48	0.48
	350	35.91	18.15	3.94	8.10	0.69	12.73	1.3
HZ-280	200	0.30	0.16	0.14	0.00	0.00	0.14	-
	250	0.78	0.49	0.19	0.00	0.00	0.19	-
	300	3.97	1.94	1.08	0.46	0.00	1.54	0.30
	350	18.78	8.41	5.01	3.60	0.00	8.62	0.97

[a] xylenes, Toluene and ethyltoluenes.

Table 4.4 reports the product distribution for ethylation of EB with ethanol over HZSM-5 samples being investigated in this study. The ethylation experiments were conducted using 1:1 EB to ethanol molar ratio and at different reaction temperatures and contact times. The analysis shows that the products are still the same as observed during

disproportionation, only the conversion of EB and the product compositions are significantly changed in case of the EB ethylation with ethanol. A small amount of triethylbenzene was found in disproportionation runs. No such product was detected in the EB ethylation with ethanol. The following sections present the effects of SiO_2/Al_2O_3 ratios along with temperature and contact time on conversion and product selectivity during both the disproportionation and ethylation of EB.

Table 4.4: Product distribution (wt%) of ethylbenzene ethylation reaction on HZSM-5 with different Si/Al ratio at 20 s reaction time.

Catalysts	Temp (°C)	EB conv. (%)	Product Yield (%)					
			Benzene	*p*-DEB	*m*-DEB	*o*-DEB	Total-DEB	Others[a]
HZ-27	200	7.47	1.48	3.58	2.37	0.13	6.08	0.64
	250	21.14	5.26	5.68	5.49	0.34	11.51	2.27
	300	34.80	10.25	5.32	6.04	0.34	11.71	6.09
	350	35.72	13.92	3.06	4.42	0.36	7.85	8.04
HZ-55	200	15.21	1.05	5.14	10.72	0.71	16.58	0.94
	250	28.80	4.25	6.40	12.86	0.94	20.20	2.91
	300	38.30	8.52	5.03	10.66	1.13	16.82	5.59
	350	44.08	15.10	2.39	4.88	0.96	8.23	9.07
HZ-80	200	17.41	0.59	6.24	9.60	0.69	16.54	0.52
	250	29.25	2.02	8.07	15.44	1.21	24.72	1.45
	300	40.57	4.86	8.90	18.13	1.80	28.83	2.98
	350	43.76	6.88	7.95	16.90	2.02	26.87	4.20
HZ-150	200	11.57	0.29	5.31	4.54	0.33	10.17	0.43
	250	26.30	1.61	8.20	13.09	0.70	21.99	1.41
	300	36.15	4.49	8.02	15.09	1.02	24.13	3.37
	350	34.11	9.59	3.86	8.19	0.96	13.01	6.16
HZ-280	200	1.30	0.00	1.06	0.11	0.00	1.17	-
	250	5.00	0.00	3.22	0.71	0.00	3.94	-
	300	14.71	0.61	12.28	4.80	0.00	17.08	0.59
	350	27.20	3.51	8.32	6.84	0.19	15.35	2.28

[a] xylenes, Toluene and ethyltoluenes.

4.1.3 Conversion of Ethylbenzene (EB)

Figure 4.3 compares the EB conversions over various SiO_2/Al_2O_3 containing HZSM-5 catalysts at 250 °C in the CREC Riser Simulator. One can see that both in ethylation and disproportionation, the EB conversion on HZ-280 catalyst was much lower compared to the other catalyst samples which is mainly due to the very low acidity of this catalyst sample. For all the five HZSM-5 samples the EB conversion in ethylation was much higher than disproportionation.

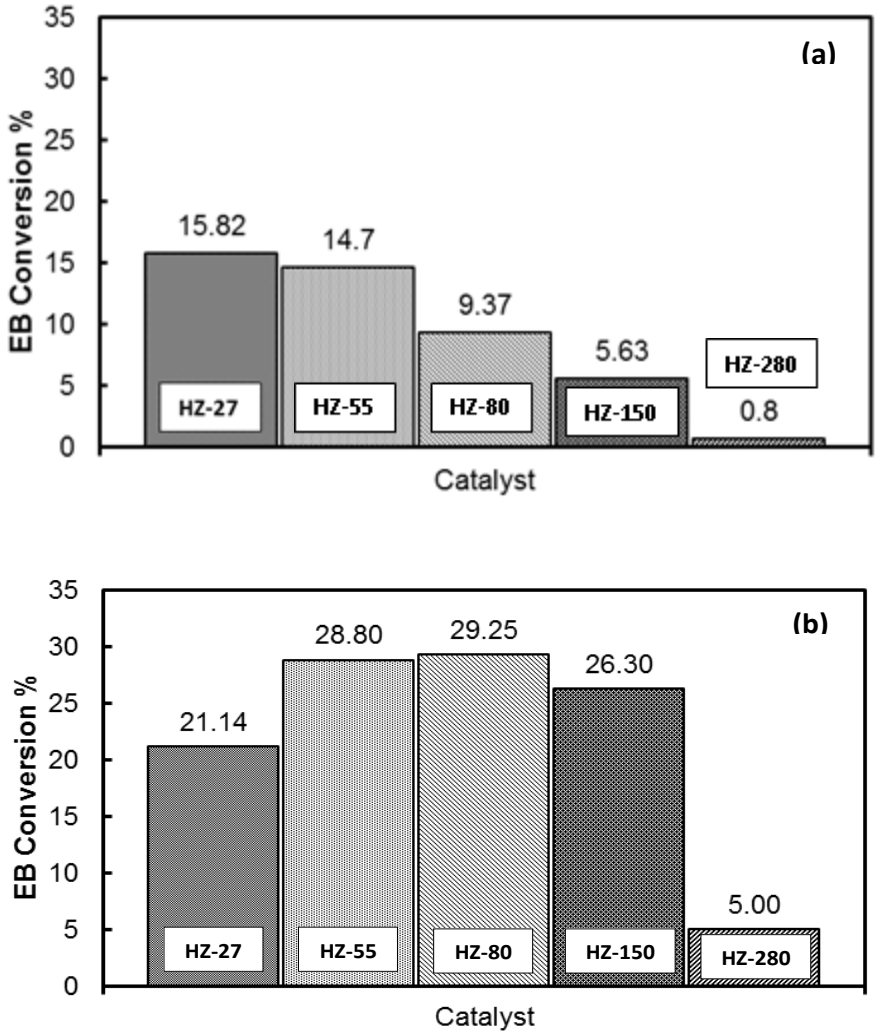

Figure 4.3 EB conversion at temperature of 250 °C and 20 sec contact time for a) EB disproportionation and b) EB ethylation over different catalysts.

When the EB conversions were plotted against temperature, it clearly shows that with increasing reaction temperature the conversion of EB increased (Figure 4.4). At temperatures higher than 300 °C the EB conversion in both the disproportionation and ethylation are comparable. This suggests that above 300 °C temperature higher amount of EB adsorbs on the on the Brönsted acid sites which favors the disproportionation [56, 57]. As a result, the overall conversion of EB in the disproportionation is increased and reached to the level of EB ethylation. For the same reason the HZSM-5 samples with higher acidity (lower SiO_2/Al_2O_3 ratios) displayed higher EB conversion in the disproportionation reaction runs than those of the lower acidic catalyst samples. The proportional relationship between the temperature and the EB conversion also suggests that under the studied range both disproportionation and ethylation reactions were away from the thermodynamic equilibrium.

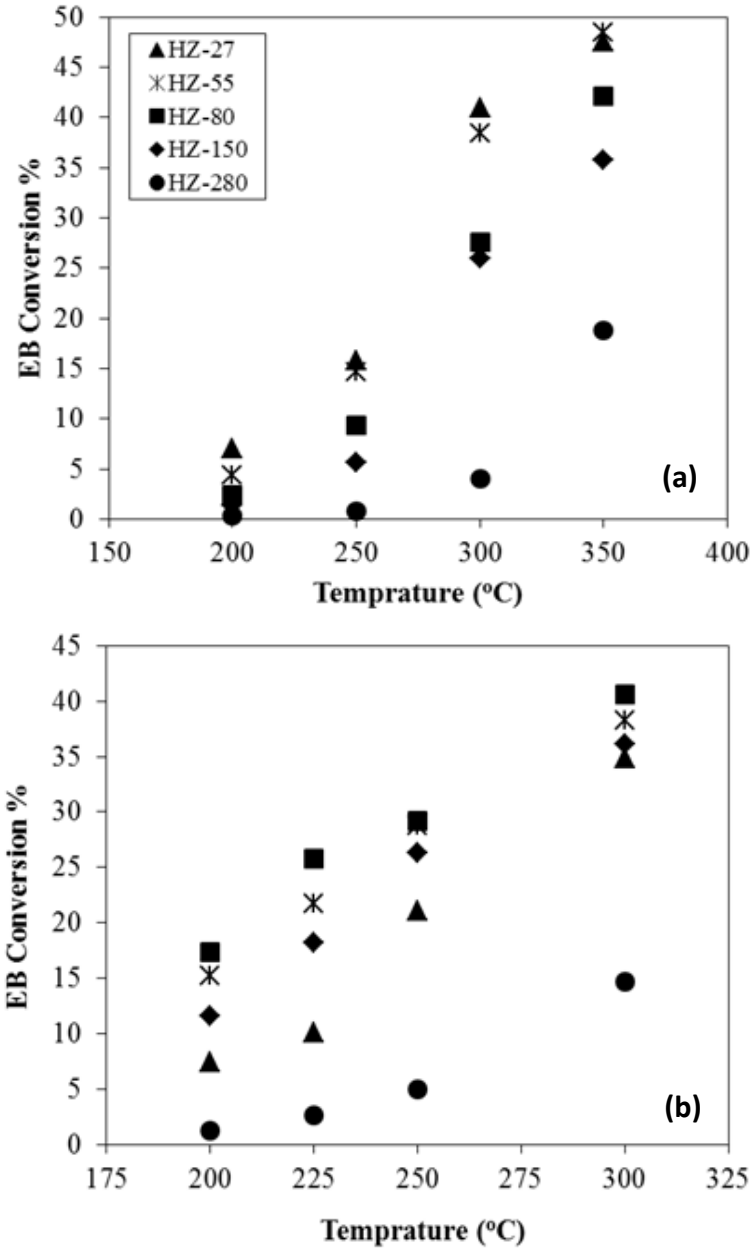

Figure 4.4. Variation of EB conversion with temperature at 20 s contact time, comparison between different catalysts for a) EB disproportionation reaction and b) EB ethylation reaction.

Figure 4.5 displays the comparison of the EB conversions at different reaction times and at constant temperature of 300 ºC. As expected, both the disproportionation and ethanol alkylation reactions, shows increasing trend with increasing the contact time. When compared among the different HZSM-5 catalysts, the higher acidic catalyst (SiO_2/Al_2O_3 = 27 and 55) displays higher conversion in disproportionation reaction compare to the other lower acid catalysts, while for ethylation reaction the EB conversion for high acid catalyst shows lower EB conversion than low acidic catalysts. Excessive acid sites and the absence of the competition for active sites between ethanol and EB favor this higher EB conversion during disproportionation. Again, due to very low acidity the HZ-280 sample shows very low EB conversion.

When compared the performance of three HZSM-5 catalysts in ethylation, the sample with SiO_2/Al_2O_3 = 80 displays superior activity. This is possibly due to the appropriate balance between the availability of strong acidic sites (11 %) along with the total acidity (0.354 mmol/g) as found in the NH_3-TPD study (Table 4.2). The sample, SiO_2/Al_2O_3 = 27 with higher total acidity (0.73 mmol/g) contains only small percentage of strong acidic sites (2 %), while with SiO_2/Al_2O_3 = 280 sample, 53 % of the total sites are strong acidic sites but the total acidity is very low (0.094 mmol/g). Consequently, this catalyst SiO_2/Al_2O_3 = 80 shows better performance as compared to the other HZSM-5 samples considered in this investigation.

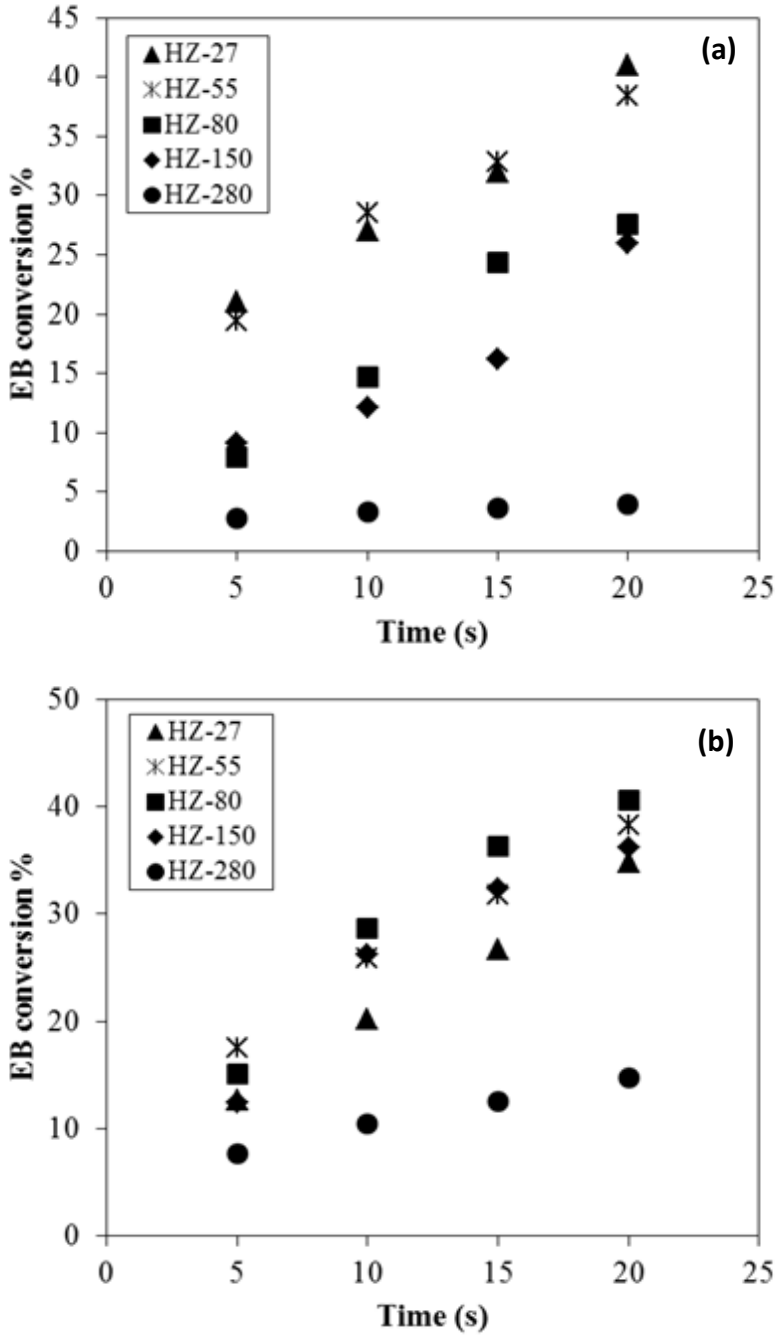

Figure 4.5. Variation of EB conversion with contact time at 300 ^{o}C, comparison between different catalysts for a) EB disproportionation reaction and b) EB ethylation reaction.

4.1.4 Selectivity of DEB and BZ

Figure 4.6 displays the selectivity of total DEB for both the disproportionation and ethylation of EB reactions using three HZSM-5 catalysts and at constant 25 % EB conversion and 300 °C temperature. HZ-280 sample is not included in Figure 4.6 given very low conversion (much less than 25 %) and negligible product yields. One can see that the DEB selectivity with all the catalysts for the ethylation reaction is almost double the selectivity in the disproportionation reaction. Among the four catalysts, the HZ-80 shows highest DEB selectivity while HZ-27 shows lowest DEB selectivity. This observation indicates that the surface acidity for the HZ-80 catalyst is suitable as compare to the other three catalysts.

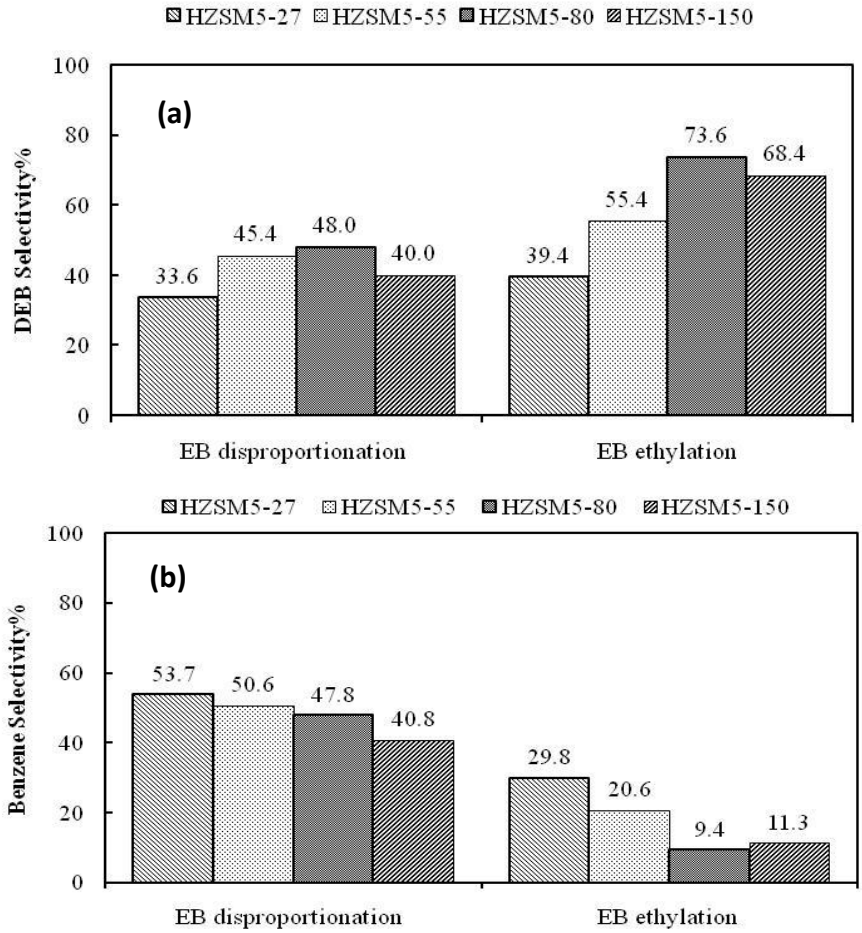

Figure 4.6 a) DEB selectivity and b) BZ selectivity for different catalysts at 25 % EB conversion and 300 ^{o}C, comparison between EB disproportionation reaction and EB ethylation reaction.

Figure 4.7 shows the DEB selectivity as function of temperature. For all catalysts the total DEB selectivity were increased with increasing reaction temperature. This trend was expected given all the experiments were conducted relatively at lower temperature (350 ºC maximum). Previous studies demonstrated that at high reaction temperature (above 400 ºC) the selectivity of DEB start to decrease due to the secondary cracking of product DEB. Al-Khattaf [59] showed that with increasing reaction temperature the selectivity of DEB reaches to maximum point then starts to decrease. The decrease in selectivity of DEB at high temperature was due to the increasing role of other reactions such as cracking and transalkylation at higher temperatures. Similar behaviors for DEB selectivity with temperature was reported by Halegeri and Das [60] and Sharnappa et al. [61, 62]. As reaction temperature increases, EB conversion and benzene selectivity increase while DEB selectivity decreases. This finding can be further confirmed by comparing the benzene (BZ) selectivity during the disproportionation and ethylation of EB. Expectedly, the benzene selectivity was drastically decreased in presence of ethanol during the ethylation of EB as the benzene selectivity was very high in the disproportionation reaction. Therefore, ethylation, is more favored, due to the nature of the disproportionation reaction where 2 mol of EB disproportionate to give 1 mol each of DEB and Benzene. Effects of contact time on the DEB selectivity is reported in Figure 4.8. For all catalysts the DEB selectivity increased with the increase of contact time. However, increments with the SiO_2/Al_2O_3 = 80 catalyst is significantly higher than the other HZSM-5 catalyst samples.

When the DEB/BZ ratios were calculated for different temperature and 20 s contact time, it was noticed that depending on the reaction temperature the DEB/BZ

ratios varies between 0.4 and 0.7. The lowest value was found for the HZSM-5 sample containing highest acidity (Si/Al = 27). Although, ideally the DEB/BZ molar ratio should be equal to 1, the discrepancy is mainly due to the cracking reaction which produces excess benzene as reflected by the lowest value for the catalyst with highest acidity. Also, the presence of some minor side products (such as toluene, xylene, and triethylbenzene) that are not included in the ratio contributed to the error.

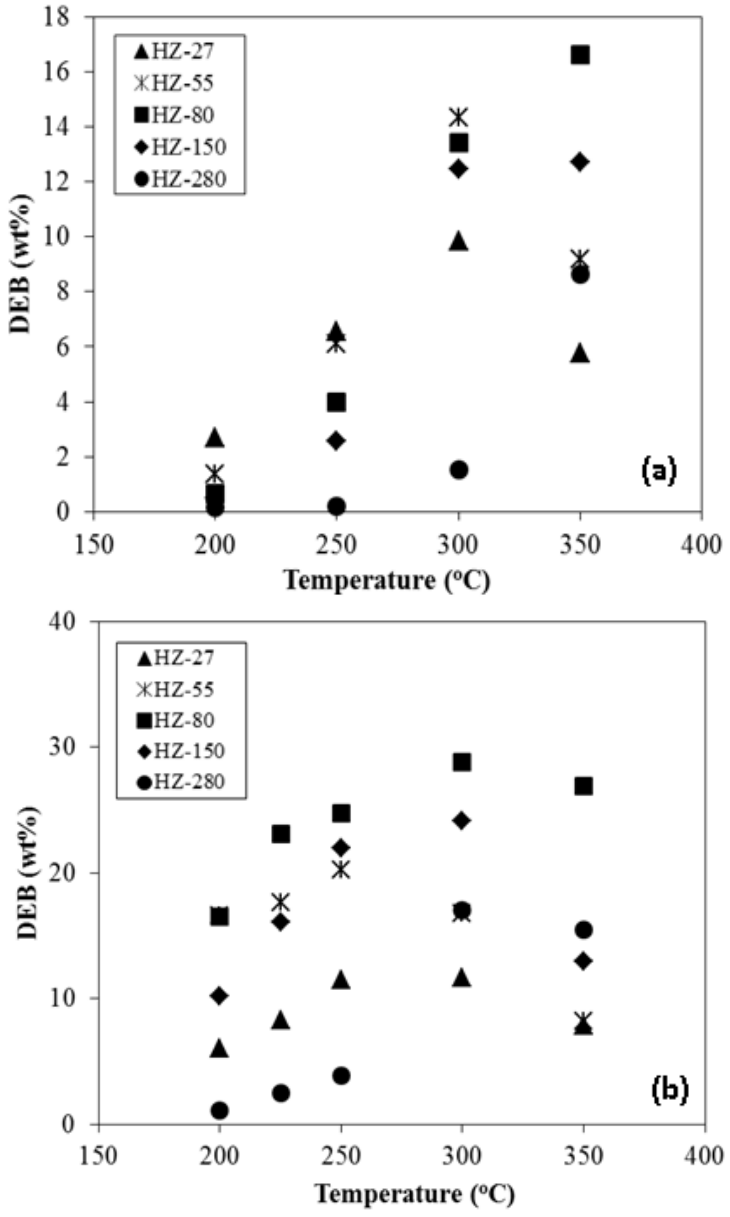

Figure 4.7 Variation of DEB yield with temperatures for a) EB disproportionation and b) EB ethylation at 20 sec, comparison between different catalysts.

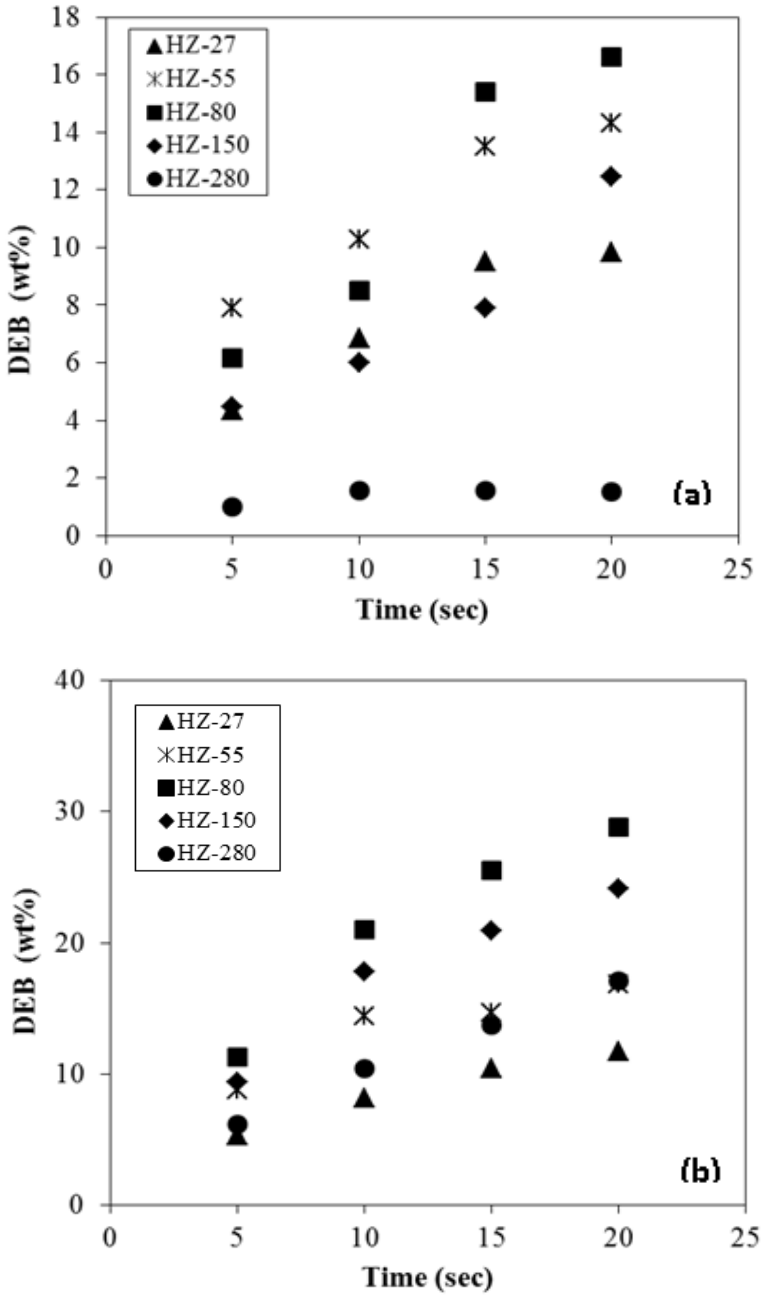

Figure 4.8 Variation of DEB yield with contact time at 300 ^{o}C for a) EB disproportionation and b) EB ethylation, comparison between different catalysts.

4.1.5 Selectivity of p-DEB

Figure 4.9 shows the p-DEB selectivity (% p-DEB/total DEB) for different HZSM-5 samples at various EB conversions and 300 °C temperature. The selectivity of HZ-280 sample was not included in Figure 4.9 given its very low product yields and low EB conversions at 300 °C. One can see in this figure especially at high temperature (also in Table 4.3 and Table 4.4) that the distribution of DEB isomers m-DEB/p-DEB/o-DEB is approximately 6:3:1, respectively. Asrenova-Hartel et al. [36, 43] reported similar observations using a H-Y zeolite catalyst. It is interesting to see that low acidity catalysts HZ-55, HZ-80 and HZ-150, regardless of disproportionation and ethylation of EB the p-DEB selectivity is almost constant at all conversion level. The stable p-DEB selectivity was also due to the lack of excessive acid sites with these catalysts. It is hypothesized that the available acid sites are just sufficient to produce p-DEB (which is the first product) and there are no further isomerization or cracking over this catalysts especially with low temperature and small contact time. For HZ-280 catalyst high p-DEB selectivity was observed (Table 4.3, 4.4) because of its low acidity lead to minimize the isomerization of p-DEB to m-DEB. On the contrary, the p-DEB selectivity for high acid catalyst (HZ-27) decreases with increase the conversion in both disproportionation and ethylation of EB. The major reason for the decreasing p-DEB selectivity is the isomerization of the para isomer to meta isomer at high conversion. Also, the secondary cracking of p-DEB to produce benzene could be another reason for the decreasing p-DEB selectivity. In the case of disproportionation with the high acidic HZ-27 catalyst, availability of abundant acidic sites at the outer surface of the catalyst helps for isomerization of p-DEB as well as cracking of both the reactant EB and product DEB. As

a result, the p-DEB selectivity was decreased with conversion. However, in the case of ethylation with ethanol, the isomerization of the p-DEB is most likely the main reason for decreasing the p-DEB selectivity using the HZ-27 catalyst given the fact the benzene selectivity is very low indicating minimal cracking of feed and product. This result further indicates the significance of the ethyl group transfer.

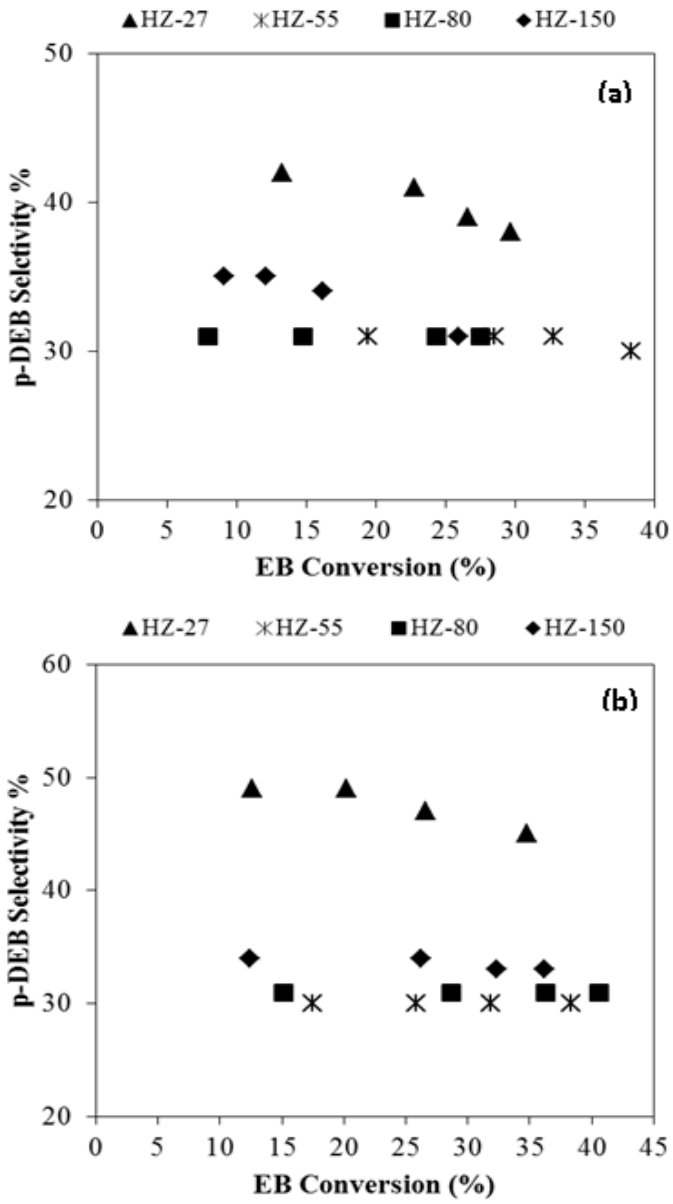

Figure 4.9. Variation of p-DEB selectivity with EB conversion at 300 ^{o}C for a) EB disproportionation and b) EB ethylation, comparison between different catalysts.

According to previous studies acidity and MFI crystal size are two important parameters that influence p-DEB selectivity over HZSM-5 catalysts [34]. Generally, low acidity and larger crystal sizes (longer diffusion length) favor the p-DEB selectivity. In the context of the present study the sample were modified to vary the acidity keeping the crystal size almost same. Therefore, the low acidic catalysts showed better and stable p-DEB selectivity. Mishin et al [26] showed that formation of very strong acid sites caused by an increasing contribution from isolated Al atoms in the framework seems to be the reason for the enhanced catalytic activity of dealuminated zeolite samples. W.-H. Chen et al. [27] reported the effects of surface modification on the para-selectivity of modified HZSM-5 samples. They concluded that during the disproportionation of EB a substantial inactivation of surface active sites is inevitable in provoking substantial relative increase in para-DEB selectivity. X. Guan et al [24] also reported improved and stable p-DEB selectivity with modified (acidity) HZSM-5 samples. It was showed that very high selectivity to p-DEB (>90%) can be achieved by controlling the concentration of very strong acid sites [63, 64].

4.1.6 Kinetic modeling

Reaction kinetics of both ethylbenzene transformation and ethylation reactions are presented in this section. Mathematical models representing the rates of chemical reactions are developed based on the main product distributions observed for both reactions. As seen in section 4.1.2, under the studied reaction conditions in the context of the present study both the disproportionation and ethylation of EB in the CREC Riser Simulator gives DEB and BZ as major products containing the aromatic ring. The gaseous product predominantly ethylene but their overall composition is very low. Considering all the facts the developed model equations are based on proposed reaction schemes 1 and 2 for ethylbenzene transformation and ethylation reactions, respectively.

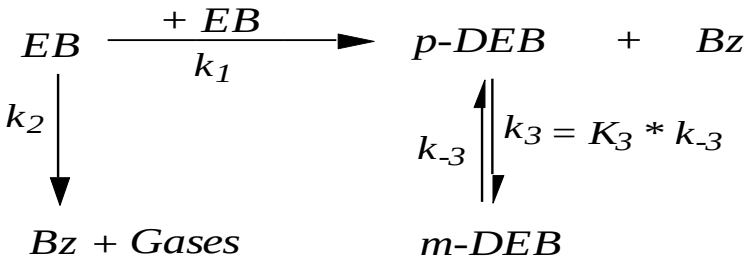

Scheme 1.Reaction network of ethylbenzene transformation

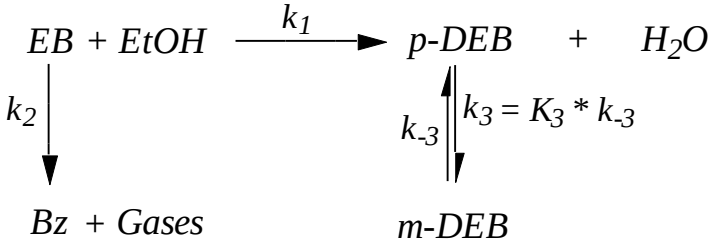

Scheme 2. Reaction network of ethylation of ethylbenzene with ethanol

In formulating the kinetic models, we assumed the ethylation reaction follows a simple second-order kinetics and a pseudo-first order reaction kinetic was assumed for disproportionation and cracking reactions. Catalyst deactivation is assumed to be a function of time on stream (TOS) and a single deactivation function was defined for all reactions. Isothermal operating conditions can also be assumed given the design of the riser simulator unit and the relatively small amount of reacting species. It is important to mention here that in model formulation the each of the DEB isomers is considered as separate products. However, given its very low yields (Table 4.3, Table 4.4) the contribution of o-DEB has been neglected. This assumption is consistent to the published literature articles, especially when the disproportionation and ethylation of EB reactions are conducted at low temperature (below 350 °C) [2, 4, 35].

- **Model development for ethylbenzene transformation**

Based on the observed product distribution, reaction scheme 1 is proposed to represent the main reacting species of the transformation reaction. Using power law model, the rate of reaction for each reacting species can be written as:

Rate of reaction for ethylbenzene

$$-\frac{V}{W_c}\frac{dC_{EB}}{dt} = (k_1 C_{EB} + k_3 C_{EB})\exp(-\alpha t) \quad (4.1)$$

Rate of reaction for benzene

$$\frac{V}{W_c}\frac{dC_B}{dt} = (k_1 C_{EB} + k_3 C_{EB})\exp(-\alpha t) \quad (4.2)$$

Rate of reaction for p-DEB

$$\frac{V}{W_c}\frac{dC_P}{dt} = (k_1 C_{EB} - k_2 C_P + k_{-2} C_m)\exp(-\alpha t) \quad (4.3)$$

Rate of reaction for m-DEB

$$\frac{V}{W_c}\frac{dC_m}{dt} = (k_2 C_P - k_{-2} C_m)\exp(-\alpha t) \tag{4.4}$$

where C_i is molar concentration of each species in the system, V is the volume of the reactor, W_c is the mass of the catalyst, t is time in seconds,k_i is the rate constant of each species, while α is the catalyst deactivation constant.

- **Model development for ethylation of ethylbenzene**

Reaction scheme 2 takes into consideration the main products of the alkylation of ethylbenzene with ethanol. The reaction network is used to develop the model equations for the kinetics of the reaction. Thus, we have:

Rate of reaction for ethylbenzene

$$-\frac{V}{W_c}\frac{dC_{EB}}{dt} = (k_1 C_{EB} C_E + k_3 C_{EB})\exp(-\alpha t) \tag{4.5}$$

Rate of reaction for p-DEB

$$\frac{V}{W_c}\frac{dC_P}{dt} = (k_1 C_{EB} C_E - k_2 C_P + k_{-2} C_m)\exp(-\alpha t) \tag{4.6}$$

Rate of reaction for m-DEB

$$\frac{V}{W_c}\frac{dC_m}{dt} = (k_2 C_P - k_{-2} C_m)\exp(-\alpha t) \tag{4.7}$$

Rate of reaction for benzene

$$\frac{V}{W_c}\frac{dC_B}{dt} = (k_3 C_{EB})\exp(-\alpha t) \tag{4.8}$$

Due to the negligible amount of benzene in the reaction product on HZ-80 and HZ-150, $k_2$and $k_3 \approx 0$.

The molar concentration C_i can be expressed in terms of weight fraction of each speciesy_i, which are the measurable variables from the chromatographic analysis, hence,

$$C_i = \frac{y_i W_{hc}}{MW_i V} \tag{4.9}$$

where W_{hc} is the weight of feedstock injected into the reactor, MW_i is the molecular weights of the species.

The rate constant was represented with the temperature dependence form of the Arrhenius equation given as:

$$k_i = k_{i0} exp\left[-\frac{E_i}{R}\left(\frac{1}{T} - \frac{1}{T_0}\right)\right] \tag{4.10}$$

where k_{i0} and E_i are the pre-exponential factor and activation energy of the reaction *i* respectively. T_0 is referred to as the centering temperature which is the average of all the temperatures for the experiment in order to reduce parameter interaction.

In order to ensure thermodynamic consistency at equilibrium, the rate constant for the isomerization reaction (p-DEB to m-DEB) in the above equation are expressed as follows:

$$\mathrm{K_2} = \frac{\mathrm{k_2}}{\mathrm{k_{-2}}} = \left(\frac{\mathrm{C_M}}{\mathrm{C_P}}\right)_{\mathrm{eq}} \tag{4.11}$$

where K_2 are temperature-dependent equilibrium constant for the isomerization reaction. However, an average value was computed for K_2, because the thermodynamic equilibrium concentrations of the DEBs remain fairly constant within the temperature range of this work.

The above models were evaluated considering that the both the disproportionation and ethylation of ethylbenzene over HZSM-5 catalyst samples were free from transport limitations. This assumption is reasonable given the fact the HZSM-5 sample has small crystallite sizes of 0.5×10^{-6} m to 2×10^{-6} m [65]. For this crystal size ranges, one can expect that the value of effectiveness factor to should be close to one. Considering this fact, the effect of diffusion has not been incorporated in the kinetics analysis. Recently, Marin et al [66] also reported the kinetic modeling ethylbenzene dealkylation over Pt promoted H-ZSM-5 zeolite catalysts by considering negligible contribution of the diffusion resistance.

- **Model Parameter Evaluation**

The mole balance equations (Eqs. 4.1-4.11) incorporating the Arrhenius relation (Eq. 4.10) were evaluated by a least square fitting of the kinetic parameters using the experimental for both the disproportionation and ethylation of EB reactions data obtained from the CREC Riser Simulator. The data points were taken at various reaction times ranging from 5-20 sec at different temperature levels. The models were evaluated by using MATLAB (ODE 45-4th order Runge-Kutta method and LSQCURVEFIT) least square fitting of the kinetic parameters. The centering temperature in the Arrhenius was taken equal to 275 °C. The optimization criteria are that all the rate constants had to be positive, the activation energies for reaction positive, all consistent with physical principles.

The parameters were determined at 95% confidence limit. Total one hundred and twelve (112) for disproportionation and one hundred and twelve (112) for ethylation of

EB reactions data points were taken for parameter estimation. Thus, total nine parameters, the degree of freedom for the model exceeded 103 and 104 (number of data points – number of parameters to be estimated), respectively. This shows that considerable experimental data were used to optimize the model parameters.

The models were discriminated based on their coefficient of determination (R^2), lower SSR (sum of the squares of the residuals, Lower cross-correlation coefficient (γ), and smaller individual confidence intervals for the model parameters. The values of the model parameters along with their corresponding 95% confidence limits (CLs) and the resulting cross-correlation coefficients are shown in Table 4.5. One should remember that the power law model as developed in Equation 1-8 are not based on the mechanism of the surface reaction. Therefore, the estimated activation energies are apparent activation energies which have combined effects various steps (adsorption of reactant-surface reaction-desorption of products) involved in the catalytic reaction.

It is noticed from Table 4.5, that in EB transformation the estimated activation energies for the cracking reaction forming benzene over all the HZSM-5 catalyst are found to be slightly higher than those for the formation of the desired product p-DEB. This result indicates that in EB transformation using HZSM-5 catalysts the cracking reaction is comparable with the desired disproportionation reaction having slight edge. This observation is consistent to the experimental selectivity data as obtained from the fluidized bed reaction runs, which shows that all the HZSM-5 catalysts are equally favors both the cracking and disproportionation to produce benzene and the desired product p-DEB. Among the five catalysts being investigated in the study, the estimated activation

energy for HZ-27 is the lowest which is in line with the highest benzene selectivity as shown in Table 4.3. When compared the activation energy for the disproportionation forming p-DEB, the HZ-27 catalyst requires the least amount of activation energy as compare to the other HZ-80 and HZ-150. This is also consistent as the acidity of this catalyst is highest among the five HZSM-5 catalysts being investigated.

Table 4.5: Estimated kinetic parameters (at 95 % confidence limit) for disproportionation and ethylation of EB over HZSM-5 catalysts with different SiO_2/Al_2O_3 ratios

Parameters	EB disproportionation			EB ethylation with ethanol		
	HZ-27	*HZ-80*	*HZ-150*	*HZ-27*	*HZ-80*	*HZ-150*
k_{01}*	2.5 ± 0.2	2.1 ± 0.1	2.3 ± 0.1	2.6 ± 0.3	4.9 ± 0.6	4.8 ± 0.4
k_{02}	330 ± 16	530 ± 98	470 ± 17	2.2 ± 0.6	146 ± 22	8.6 ± 0.4
k_{03}	0.87 ± 0.2	0.36 ±0.1	0.38 ± 0.1	0.01 ± 0.002	-	-
E_1	19.5 ± 7.0	38 ± 4.5	43 ± 5.3	25.6 ± 3.8	22.5 ± 4.4	38.4 ± 3.3
E_3	40 ± 4.4	40 ± 4.0	50 ± 8.0	78.8 ± 12.8	-	-

k_{01}, k_{02}, k_{03}: $1 \times 10^3 m^3$/kgcat.s
E_1, E_1, E_1: kJ/mol
*(for ethylation: k_{01}: 1×10^2 m^6/kgcat.s)

The scenario is completely different during the ethylation of EB with ethanol than that was observed in EB transformation (Table 4.5). As noticed in the product analysis (Section 4.1.2, Table 4.4), the majority of the EB converted into DEB and only small amount of benzene was produced. The estimated activation for the cracking reaction was very high (78.8 ± 12.8) which is consistent to the very low selectivity of benzene during

the ethylation of EB with ethanol. Therefore, in presence of ethanol, the contribution to either DEB or benzene via disproportionation (as shown in scheme 2) can be considered negligible. The much lower activation energy (Table 4.5) for the ethylation route is also consistent to the above explanation. The catalyst with SiO_2/Al_2O_3 = 80 requires the least amount of activation energy forming p-DEB compare to HZ-27 and HZ-150. This finding is also consistent to the product analysis results, which shows that highest p-DEB yield with the SiO_2/Al_2O_3 = 80 containing HZSM-5 catalyst.

The estimated kinetic parameters for the fitted parameters substituted into the developed the mole balance equation and equations were numerically solved using fourth-order-Runge-Kutta routine. Figure 4.10 and Figure 4.11, are the reconciliation plots for the EB conversion during disproportionation and ethylation, respectively. The model predicted and experimental EB conversion and products yield are compared in Figure 4.12. Both the predicted conversions and yield data fit the experimental data in an excellent manner.

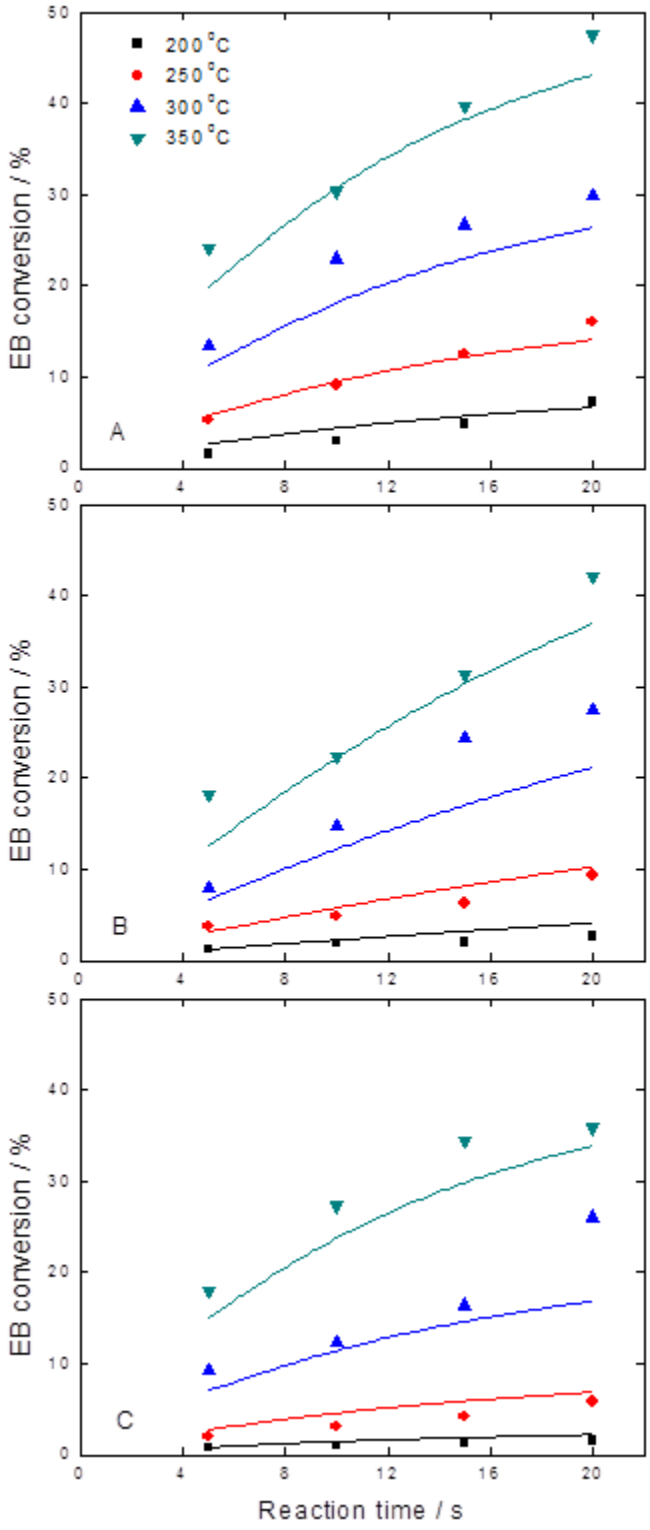

Figure 4.10. EB disproportionation reaction: Influence of reaction temperature and time on ethylbenzene conversion on HZSM-5 samples with: A) SiO_3/Al_2O_3 = 27, B) SiO_3/Al_2O_3 = 80 and C) SiO_3/Al_2O_3 = 150. Experimental data: data points, model prediction: continuous

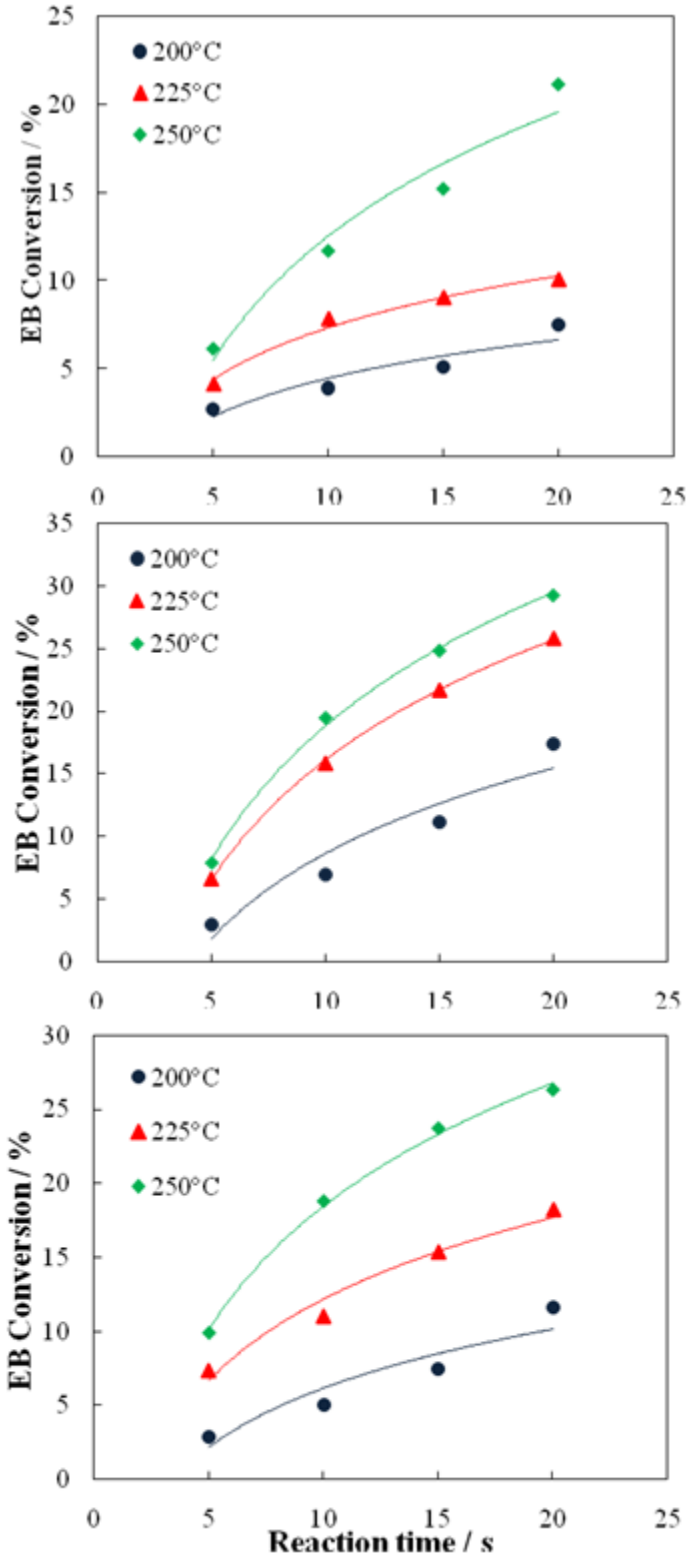

Figure 4.11. EB ethylation reaction: Influence of reaction temperature and time on ethylbenzene conversion on HZSM-5 samples with: A) SiO_3/Al_2O_3 = 27, B) SiO_3/Al_2O_3 = 80 and C) SiO_3/Al_2O_3 = 150. Experimental data: data points, model prediction: continuous

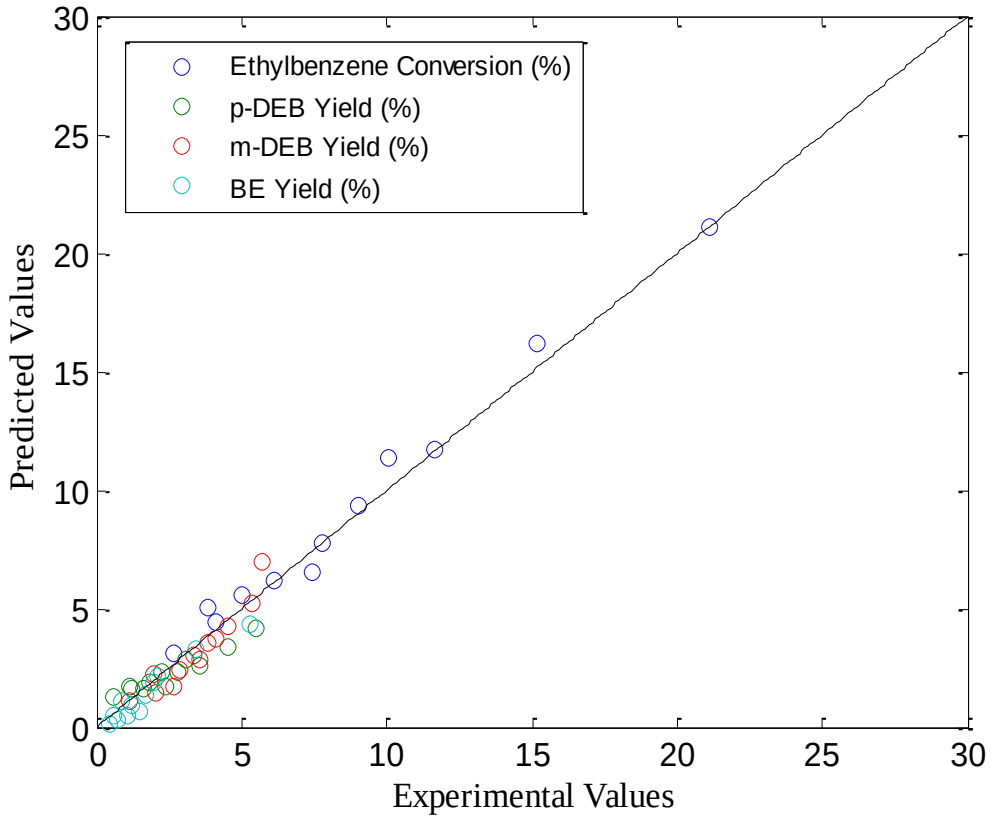

Figure 4.12. Reconciliation plot between model predictions and experimental data. Experimental data: data points, model prediction: continuous line

4.2. Effect of zeolite pore structure on ethylbenzene ethylation:

4.2.1. Physicochemical properties of the catalysts

X-ray powder patterns of all zeolites under study showed good crystallinity and characteristic diffraction lines (not shown here). The specific surface area and pore volume determined by nitrogen physisorption for the ZSM-5 and mordenite samples are listed in Table 4.6. The pyridine FTIR characterization confirmed the presence of Brönsted and Lewis acid sites. The amount and percentages of each of Brönsted and Lewis type acid sites are presented in Table 4.6. The crystal sizes of all zeolites used in this study were between 0.5 and 1 μm.

Table 4.6: Characteristics of the catalysts under study.

	ZSM-5	**Mordenite**
Si/Al ratio	150	180
Channel dimensions (Å)	5.1×5.5 and 5.3×5.6	6.5×7.0 and 2.6×5.7
Pore topology	3D, 10-rings	1D, 12 and 8-rings
BET area (m^2/g)	435	420
Pore volume (V_{micro} cm^3/g)	0.17	0.27
Lewis sites (mmol/g)	0.05 (39%)	0.002 (6%)
Bronsted sites (mmol/g)	0.08 (61%)	0.030 (94%)

4.2.2. Ethylation of ethylbenzene

As mentioned in the experimental section, ethylation of EB experiments were conducted in a CREC Riser Simulator under fluidized bed conditions. The ethylation experiments were conducted using 1:1 EB to ethanol molar ratio and at different reaction temperatures and contact times. Table 4.7 presents the product distribution of the ethylation of EB over the HZ-150 and MOR-180 samples after 20 seconds reaction time at three levels of reaction temperatures (250, 300 and 350°C). One can see that at all temperature levels diethylbenzene (DEB) are the main products. A small amount of triethylbenzene (TEB) was observed using MOR-180 catalysts. No such product was detected in the EB ethylation over HZ-150. Among the DEB isomers p-DEB and m-DEB were dominant while a small amount of o-DEB was also detected under the present experimental conditions. A small amount of benzene was also detected over both catalysts as a result of EB disproportionation. The other hydrocarbon products such as toluene and gaseous hydrocarbons are negligible. The following sections present the effects of zeolites pore size along with temperature and contact time on conversion and product selectivity during EB ethylation.

Table 4.7: Product distribution (wt%) of ethylbenzene ethylation over HZ-150 and MOR-180 at different temperature level and 20 s reaction time.

Catalysts	Temp (°C)	EB conv. (%)	Product Yield (%)							
			Benzene	*m*-DEB	*p*-DEB	*o*-DEB	Total-DEB	TEB	Gases	Others[a]
HZ-150	250	26.30	1.61	13.09	8.20	0.70	21.99	0.00	1.24	1.45
	300	36.15	4.49	15.09	8.02	1.02	24.13	0.00	4.04	3.48
	350	34.11	9.59	8.19	3.86	0.96	13.01	0.00	5.24	6.27
MOR-180	250	30.89	1.36	11.51	4.87	2.21	18.59	8.19	1.83	0.93
	300	41.31	1.92	15.23	6.93	2.13	24.29	10.91	2.76	1.43
	350	42.82	5.52	12.69	5.84	1.80	20.33	4.73	5.88	6.36

[a] xylenes, Toluene and ethyltoluenes.

4.2.3 Conversion of ethylbenzene (EB) and ethanol (EtOH)

Ethylbenzene alkylation with ethanol can be considered as an electrophilic substitution on the aromatic ring, and over acidic zeolites it is commonly considered as proceeding via a carbonium ion-type mechanism [33]. Figure 4.13 compares the conversions of EB and EtOH during the ethylation reaction over medium and large pore zeolite samples at different temperature level. One can see that in both HZ-150 and MOR-180, EtOH conversion was much higher compared to EB conversion at any temperature although equal molar amount of EtOH and EB was injected as feed. The main reason for the higher EtOH conversion is the primary and secondary alkylation reactions which consumes the additional EtOH molecules. Figure 4.13 also shows that EtOH conversion was almost in the same higher level over both the HZ-150 and MOR-180 samples.

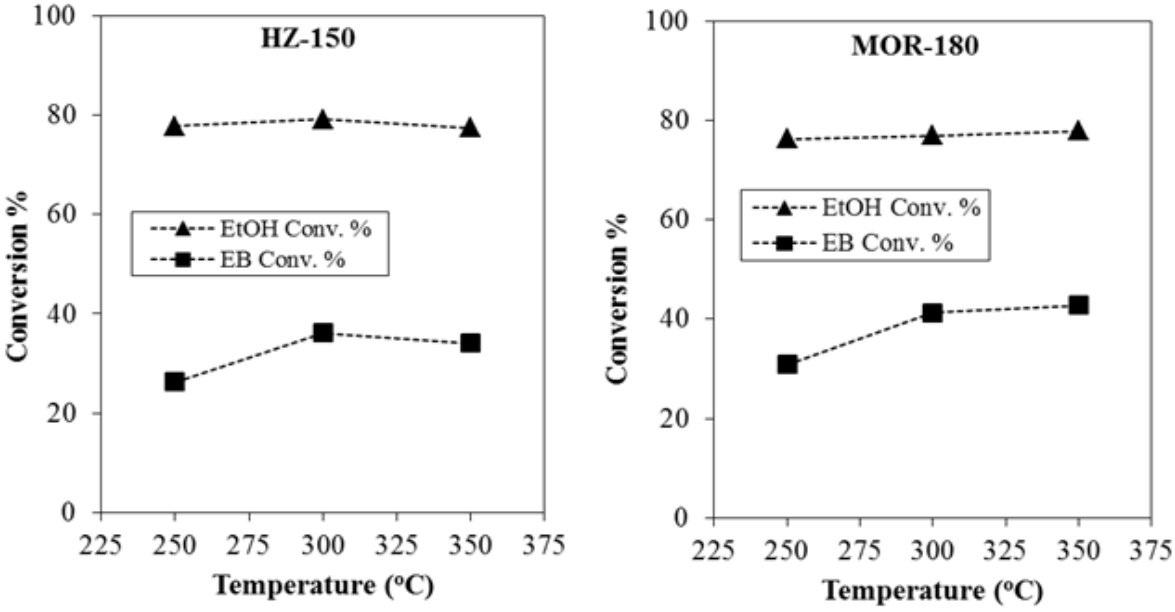

Figure 4.13. Effect of temperature on the ethylbenzene and ethanol conversions in the ethylation of ethylabenzene over medium pore zeolite (HZ-150) and large pore zeolite (MOR-180).

4.2.4 Products yield and selectivity

Figure 4.14 displays the products yield for ethylation of EB for the two catalysts at various temperatures and at 20 second contact time. One can notice that over all catalysts with increasing reaction temperature the yield of DEB reaches to maximum point at 300^{o}C then starts to decrease. The decrease in yield of DEB at high temperature is due to cracking and secondary alkylation at higher temperatures. Similarly, TEB yield increase with temperature until reach to the maximum then decrease at high temperature. A similar observation for DEB selectivity with temperature was reported by Halegeri and Das [60] and Sharnappa et al. [61, 62] EB conversion and benzene selectivity increases, while DEB selectivity decreases with reaction temperature. On the other hand benzene yield was increased with increasing the reaction temperature for both catalysts. This observation suggests that at high temperature a favorable condition attains for EB disproportionation to benzene and DEB, especially with the medium pore zeolite HZ-150.

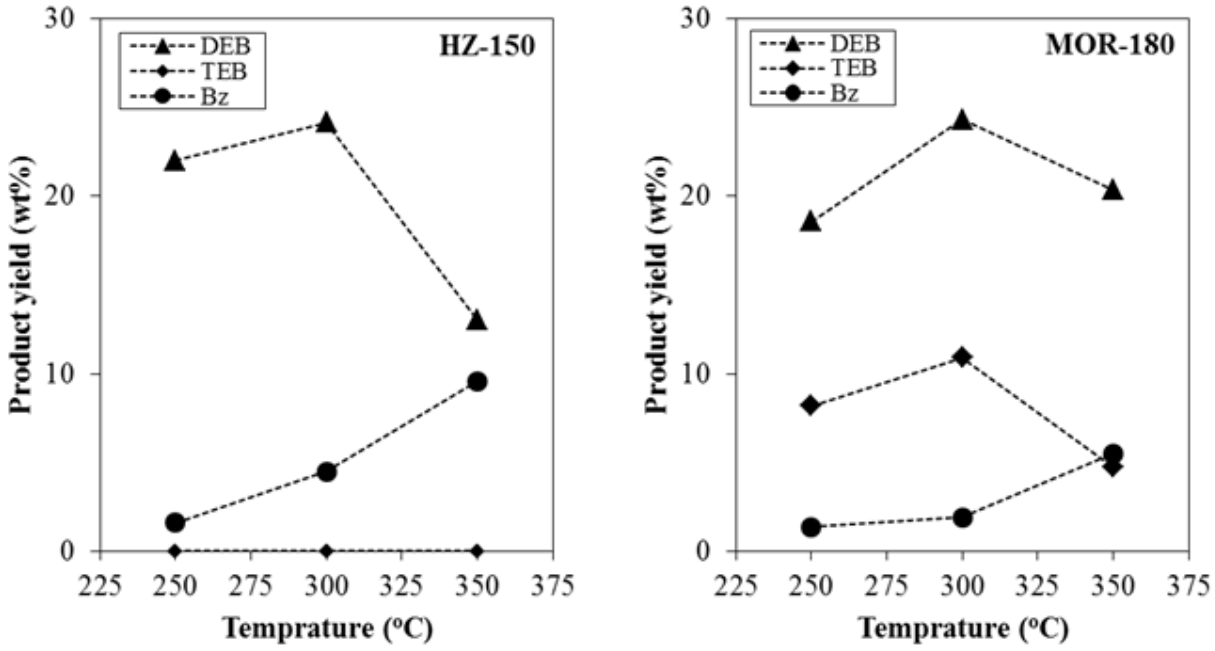

Figure 4.14. Product yield for the ethylbenzene ethylation over MOR-180 and HZ-150 catalyst at different temperature and 20 s contact time.

Figure 4.15 summarizes the products selectivity of the alkylation of ethylbenzene with ethanol over medium and large pore zeolite catalysts at similar level of conversion (EB conv. = 20%). One can see that products selectivity is comparable over the two catalysts. Diethylbenzene was the main product observed over both catalysts which might be attributed to its ease of diffusion without steric hindrance through the pores of the catalysts. The primary alkylation reaction forms DEB, while the secondary alkylation led to formation of TEB. Triethylbenzene (TEB) was formed only over MOR-180 as shown in Figure 4.15 and Figure 4.16 and no TEB was observed over HZ-150 catalyst. This result is not surprising, since HZ-150 is medium pore size (~0.6 nm) restrict the formation of large molecules such as TEB due to steric restrictions, on the other hand, the large pore size MOR-180 (~0.7 nm) favors secondary alkylation reactions which is allow the formation of TEB without diffusional resistance. Regarding benzene selectivity,

one can see in Figure 4.15 very low selectivity of benzene in ethylation of ethylbenzene. Comparing the two samples HZ-150 shows higher benzene selectivity. The effect of contact time on DEB yield is reported in Figure 4.17. For all catalysts DEB yield increased with the increase in contact time. However, increment with HZ-150 catalyst is slightly higher than the MOR-180 especially at low temperature.

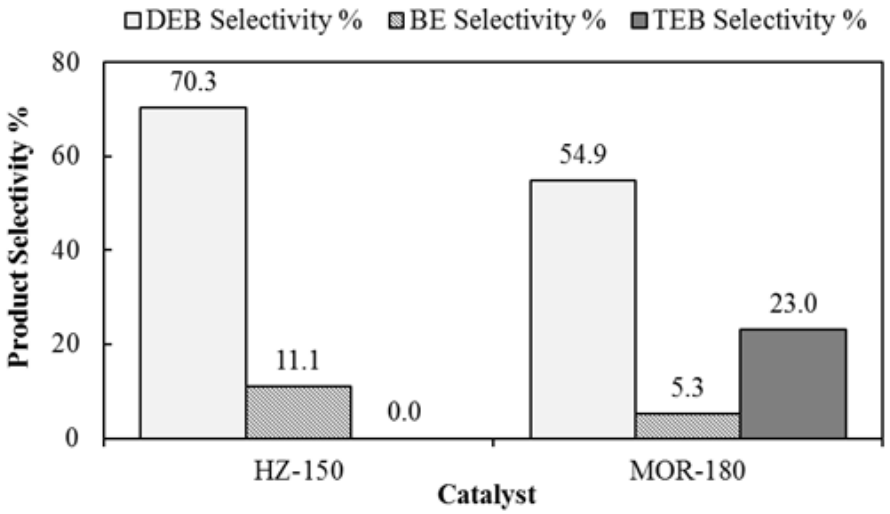

Figure 4.15. Comparison of the product selectivity in the ethylbenzene ethylation over medium pore zeolite (HZ-150) and large pore zeolite (MOR-180) (T = 300°C, EB conversion = 20%).

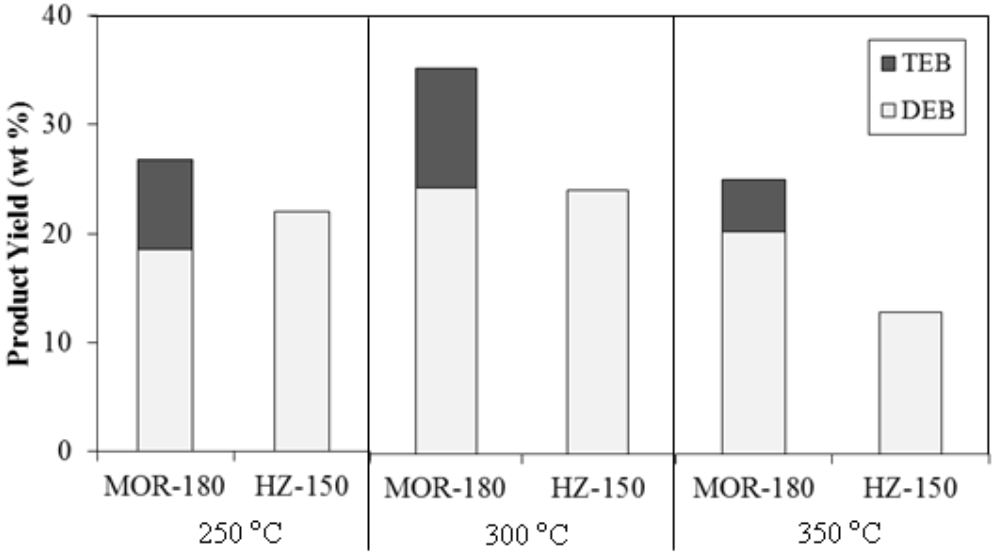

Figure 4.16. Effect of temperature on the yield of DEB and TEB for ethylbenzene ethylation. Comparison between medium and large pore zeolites (contact time = 20 s).

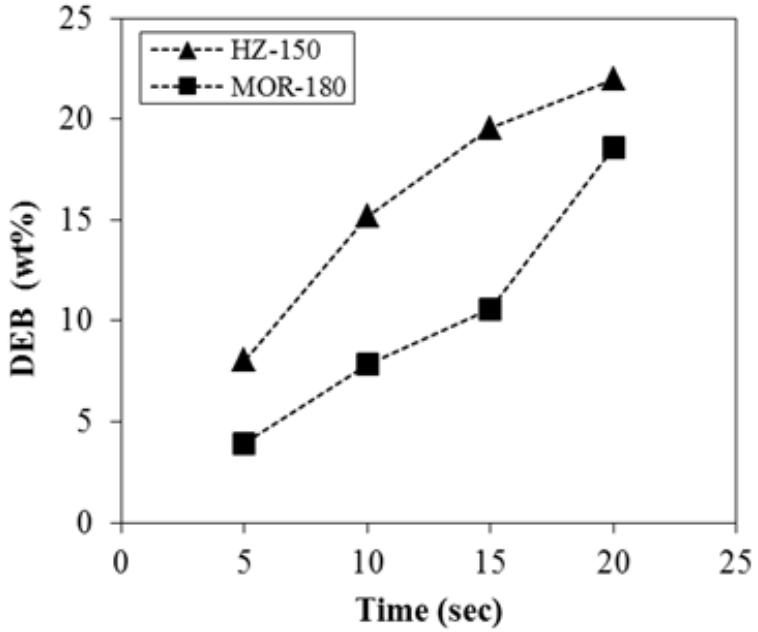

Figure 4.17. Effect of contact time on the yield of DEB in the ethylbenzen ethylation. Comparison between medium and large pore zeolites (T = 250 ^{o}C).

The results show that HZ-150 gave higher value of p-DEB selectivity compare to MOR-180 especially at low temperature. This can be explained by the difference between the structures of the two zeolites; because medium pore zeolites exhibiting channels with dimensions of about 0.55 nm have led to shape selectivity in the processing of alkylaromatic, particularly with respect to para isomer of diethylbenzene, while over large pore zeolite most of the p-DEB selectivity was closed to the thermodynamic equilibrium value. This is because MOR allows the isomers to freely move without diffusional constraints.

4.2.5. Kinetic mechanism of ethylbenzene ethylation

In this section the details of the kinetic mechanism of ethylbenzene alkylation with ethanol over medium and large pore zeolites are presented. As seen in section 4.2.2, under the studied reaction conditions in the context of the present study ethylation of EB over HZ-150 and MOR-180 in the CREC Riser Simulator gives DEB and TEB as major products while a small amount of benzene was also obtained. The other possible products such as toluene, gaseous hydrocarbons and xylenes are negligible. Benzene can be produced through cracking or disproportionation of EB. However, given that ethylation reactions are conducted at low temperature level and the amount of cracking gas in the products was found as small amounts; this suggests that the benzene is mainly produced via the disproportionation reaction. Considering all the facts following reaction scheme is considered in the kinetic modeling:

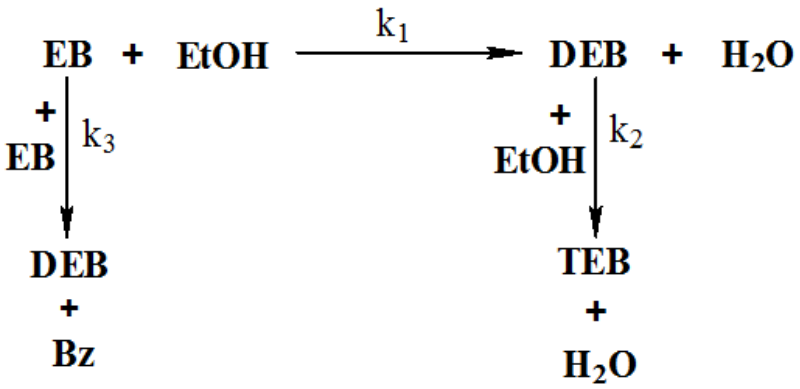

Reaction network of alkylation of ethylbenzene with ethanol

In formulating the kinetic models, we assumed a lumped model (all DEB isomers as one product), given that DEB isomers are at equilibrium (m-DEB/p-DEB/o-DEB = 6:3:1) in ethylation of ethylbenzene reactions. This assumption allowed us to estimate the

set of kinetics parameters which successfully predicted the DEB selectivity. Using the equilibrium ratios one can easily determine the selectivity of the various DEB isomers.

In the open literature there are many kinetic models have been used to describe the catalytic alkylation of aromatics, most of these models are based on Langmuir-Hinshelwood or Eley-Rideal mechanisms. The kinetic study of Corma et al [48] on alkylation of benzene with propylene over zeolites MCM-22 show that the reaction follows Eley-Rideal mechanism; propylene adsorbed on the catalyst surface while benzene react from the gas phase. A similar reaction mechanism was considered for toluene methylation and studied by Sotelo et al. [67] Another example is the alkylation of benzene with methanol in the work of Smirniotis et al. [49] It was found that the reaction mechanism follows Langmuir-Hinshelwood mechanism over medium pore zeolite and Eley-Rideal mechanism over large pore zeolite. Over large pore zeolites Smirniotis et al. [49] suggested that the aromatic molecule can easily diffuse in the zeolite pores and react from the gas phase with the adsorbed alkylating agent. The rate determining step in most of these models is the reaction between the adsorbed alkylating agents and the aromatics on the gas phase.

- **Model development for ethylbenzene ethylation**

Based on the above discussion and the analysis of the kinetic data Langmuir–Hinshelwood mechanism with surface reaction control has been proposed for ethylation of ethylbenzene over medium and large pore zeolites according to the following scheme:

Adsorption of ethanol (EtOH)

$EtOH_{(g)} + X \leftrightarrow EtOH - X$

Adsorption of ethylbenzene (EB)

$EB_{(g)} + X \leftrightarrow EB - X$

Surface reactions

$EB - X + EtOH - X \rightarrow DEB - X + H_2O - X$

$DEB - X + EtOH - X \rightarrow TEB - X + H_2O - X$

$2EB - X \rightarrow DEB - X + BZ - X$

Desorption of products

$DEB - X \leftrightarrow DEB_{(g)} + X$

$TEB - X \leftrightarrow TEB_{(g)} + X$

$BZ - X \leftrightarrow BZ_{(g)} + X$

$H_2O - X \leftrightarrow H_2O_{(g)} + X$

Accordingly for the proposed reaction scheme the reaction rates were formulated as follows:

$$r_1 = k_1 \theta_{EB} \theta_{Et} \quad (4.12)$$

$$r_2 = k_2 \theta_{DEB} \theta_{Et} \quad (4.13)$$

$$r_3 = k_3 \theta_{EB}^{\ 2} \tag{4.14}$$

and the fractional coverage of ethylbenzene, ethanol, and diethylbenzene can be expressed as:

$$\theta_{EB} = \frac{K_{EB} C_{EB}}{(1 + K_{Et} C_{Et} + K_{DEB} C_{DEB} + K_{EB} C_{EB} + K_{TEB} C_{TEB} + K_{Bz} C_{Bz})} \tag{4.15}$$

$$\theta_{Et} = \frac{K_{Et} C_{Et}}{(1 + K_{Et} C_{Et} + K_{DEB} C_{DEB} + K_{EB} C_{EB} + K_{TEB} C_{TEB} + K_{Bz} C_{Bz})} \tag{4.16}$$

$$\theta_{DEB} = \frac{K_{DEB} C_{DEB}}{(1 + K_{Et} C_{Et} + K_{DEB} C_{DEB} + K_{EB} C_{EB} + K_{TEB} C_{TEB} + K_{Bz} C_{Bz})} \tag{4.17}$$

It is important to note here that the adsorption of water is negligible. Hence, K_{H2O} equals to zero in the above surface coverage expressions.

The mole balance of the reactant and product species during the ethylbenzene ethylation in the fluidized CREC Riser Simulator provides the direct relation among the intrinsic reaction rates of the individual reaction steps and the concentrations of involved species. In mole balance, the following assumptions were considered:

i. The ethylation reaction is irreversible.
ii. The contribution of thermal reaction considered to be negligible. This validity of the assumption was confirmed by conducting thermal runs without catalysts.
iii. Isothermal reaction conditions can be assumed given the amount of reactant injected in each run is very small. Therefore, the contribution of heat of reaction is

very little. This is confirmed by the negligible temperature change observed during the reaction runs.

iv. A single effectiveness factor was considered for ethylbenzene, diethylbenzene and triethylbenzene.

v. The effectiveness factor η was assumed to be unity. This assumption was made based on the fact that ZSM-5 sample have crystallite sizes of 0.5×10^{-6} m to 2×10^{-6} m [65]. For this crystal size ranges, one can consider negligible contribution of the diffusion resistance. A similar consideration was made by Marin and his co-workers [66], showed that the mordenite with a larger pore opening should not have any diffusion limitations.

Taking into account of the above assumptions the mole balance of various species gives the following set of differential equations:

Rate of disappearance of ethylbenzene (EB)

$$-\frac{V}{W_C}\frac{dC_{EB}}{dt}=\eta\left(r_1+r_3\right)\varphi \tag{4.18}$$

Rate of formation of diethylbenzene (DEB)

$$\frac{V}{W_C}\frac{dC_{DEB}}{dt}=\eta\left(r_1-r_2+r_3\right)\varphi \tag{4.19}$$

Rate of formation of triethylbenzene (TEB)

$$\frac{V}{W_C}\frac{dC_{TEB}}{dt}=\eta\, r_2\,\varphi \tag{4.20}$$

where C_i is molar concentration of each species in the system, V is the volume of the reactor, W_c is the mass of the catalyst, t is time in seconds, φ is the apparent deactivation

function, η is an effectiveness factor. The molar concentration C_i can be expressed in terms of weight fraction of each species y_i, which are the measurable variables from the chromatographic analysis, hence,

$$C_i = \frac{y_i W_{hc}}{MW_i V} \tag{4.21}$$

where W_{hc} is the weight of feedstock injected into the reactor, MW_i is the molecular weights of the species. The intrinsic rate constant can be expressed according to Arrhenius equation:

$$k = k_0 \, exp\left(\frac{-E}{RT}\right) \tag{4.22}$$

Previous studies suggests that the intrinsic mathematical structure of this equation introduces a very strong dependence between the parameters k_0 and E; called parameter correlation, makes the estimation of the correct values of the model parameters very difficult [68]. In order to reduce the correlation between the parameters the reaction rate constant was represented with the temperature dependence using the following reparameterization form of Arrhenius equation:

$$k_i = exp\left[A_i - B_i\left(\frac{1}{T} - \frac{1}{T_o}\right)\right] \tag{4.23}$$

where $A = ln[k_0]$ and $B = \frac{E}{R}$,

Conventionally, the temperature dependence relations of the adsorption equilibrium constants can be expressed according to the following thermodynamic relations: [69, 70]

$$K_i = \exp\left(-\frac{\Delta G^0_{ads,i}}{RT}\right) \tag{4.24}$$

where, $\Delta G^0_{ads,i}$ is the Gibbs free energy for adsorption of species *i* at standard conditions (298 K and 1 atm) which is further related to the change of enthalpy $\Delta H^0_{ads,i}$ and change of entropy $\Delta S^0_{ads,i}$ of adsorption as follows:

$$\Delta G^0_{ads,i} = \Delta H^0_{ads,i} - T\Delta S^0_{ads,i} \tag{4.25}$$

Combining Eq. (4.24) and Eq. (4.25) gives,

$$K_i = \exp\left(\frac{\Delta S^0_{ads,i}}{R} - \frac{\Delta H^0_{ads,i}}{RT}\right) \tag{4.26}$$

Alternatively, the above Equation (4.26) can be represented with the centered temperature form as:

$$K_i = exp\left[D_i - F_i\left(\frac{1}{T} - \frac{1}{T_o}\right)\right] \tag{4.27}$$

where $D = \frac{\Delta S_{ads}}{R}$ and $F = \frac{\Delta H_{ads}}{R}$.

Finally, the possible effects catalyst deactivation has been taken into account by considering a time on stream deactivation function as described in Equation (16) [71].

$$\varphi = exp(-\alpha t) \tag{4.28}$$

where, α is a constant and *t* is the time the catalyst is exposed to reaction.

- **Parameter evaluation and model discrimination**

The mole balance equations incorporating with Langmuir-Hinshelwood models for the individual reaction steps, Arrhenius relation, the temperature dependence form of the equilibrium adsorption constants and deactivation function were evaluated by a least square fitting of the kinetic parameters using the experimental data for EB ethylation reaction obtained from the CREC Riser Simulator. The experimental conversion and selectivity data points were taken at various reaction times ranging from 5-20 sec at different temperature levels. The differential equations were solved by Runge-Kutta method (MATLAB ODE 45 subroutine). On the other hand the Modified Marquad method technique (MATLAB LSQCURVEFIT subroutine) was employed for parameter estimation. The optimization criteria for the model evaluation are that all the rate constants, adsorption equilibrium constants, the activation energies and the heat of adsorption had to be positive, all consistent with physical principles. The minimum sum of squares of the residuals was set as optimization criteria which was defined by:

$$SS = \sqrt{\sum_{i=1}^{N}\left(C_{i,exp} - C_{i.th}\right)^2} \tag{4.29}$$

It was considered that the model is conversed the model function changed less than the specified tolerance of 10^{-8}.

In model discrimination, the coefficient of determination (R^2), lowest sum of the squares of the residuals (SSR), least value of the cross-correlation coefficient (γ), and minimum individual confidence intervals for the estimated model parameters.

Based on Langmuir-Hinshelwood approach along with the reaction scheme and the experimental data, the proposed model had been tested and due to the negligible amount of TEB in the reaction product on HZ-150, $k_2 \approx 0$. The initial model evaluation showed that the estimated equilibrium constant for EB was very small. In addition, ethanol has more tendencies to adsorb on the catalysts sites as compared to ethylbenzene. On the active sites the adsorbed ethanol transformed into surface ethoxy groups. These ethoxy groups interact with lightly adsorbed ethylbenzen to form diethylbenzene. Consequently, $K_{EB}\,C_{EB} << K_{Et}\,C_{Et}$, hence $K_{EB}\,C_{EB}$ can be dropped from the denominator of the specific reaction rate equations (Eq. 4.15, 4.16 and 4.17). A similar trend was observed for alkylation of toluene with isopropyl alcohol studied by Barman et. al [72]. In which, the estimated adsorption constants for the proposed model was found to be in the following order $K_{cy}>>K_{IPA}>>K_{To}$ which reflect the adsorption strength of those molecules, the large aromatic molecule strongly adsorbed on the catalyst sites compare to the small one. On the other hand given the low concentration of triethylbenzene and benzene in the product, one can expect that their adsorption equilibrium constant cannot be estimated accurately. Therefore, they are not considered in the model evaluation. Accordingly for the proposed the reaction scheme the reaction rates were reduced to the following expression:

$$r_1 = \frac{k_1 K_{EB} K_{Et} C_{EB} C_{Et}}{(1 + K_{Et} C_{Et} + K_{DEB} C_{DEB})^2} \tag{4.30}$$

$$r_2 = \frac{k_2 K_{DEB} K_{Et} C_{DEB} C_{Et}}{(1 + K_{Et} C_{Et} + K_{DEB} C_{DEB})^2} \tag{4.31}$$

$$r_3 = \frac{k_3 (K_{EB} C_{EB})^2}{(1 + K_{Et} C_{Et} + K_{DEB} C_{DEB})^2} \tag{4.32}$$

After dropping of the less prominent parameters, the models were further evaluated by using equation (19) and (20). The values of the model parameters along with their corresponding 95% confidence limits (CLs) are shown in Table 4.8 and Table 4.9. The Arrhenius and van't Hoff plots for the model parameters are shown in Figure 4.18 and 4.19, respectively, and it can be observed that the figures follow the expected Arrhenius and van't Hoff relationships. The activation energies for EB ethylation and heat of adsorption of EtOH and DEB for the two samples are reported in Table 4.8. The estimated activation energy for the formation of DEB over MOR-180 was found to be much smaller (45.2 kJ/mol) than the formation of DEB over HZ-150 (112 kJ/mol). These results are expected since MOR-180 catalyst is more favorable for the alkylation reaction of aromatics to a higher extent than HZ-150. This can be explained by the difference of the pore structure of the two samples, while HZ-150 is a medium pore zeolite containing two types of intersecting channels, near circular (0.53-0.56 nm) zigzag channels and elliptical (0.51-0.55 nm) straight chain channels and MOR-180, a one-dimensional large pore zeolite with a nominal free diameter of 0.67-0.70 nm [34].

Table 4.8: Estimated activation energies and adsorption enthalpies for ethylbenzene ethylation over HZ-150 and MOR-180.

Parameters (kJ/mol)	**MOR-180**	**HZ-150**
E_1	45.2 ± 6.5	112 ± 7.5
E_3	88.7 ± 10	163 ± 13
$-\Delta H_{Et}$	32.4 ± 7.3	52.4 ± 7.3
$-\Delta H_{DEB}$	85.3 ± 10.2	67.7 ± 7.5

Table 4.9: Estimated Adsorption constants for ethylbenzene ethylation over MOR-180 and HZ-150.

Temperature	**MOR-180**		**HZ-150**	
(K)	K_{DEB}	K_{Et}	K_{DEB}	K_{Et}
600	0.452	0.745	0.534	0.617
623	0.240	0.586	0.324	0.419
650	0.121	0.452	0.188	0.275
673	0.071	0.368	0.123	0.198

One may be interested to make a comparison between the estimated parameters with values available in the open literature. Unfortunately, there are no such data available in the open literature that can be directly compared with our results of the activation energies and adsorption enthalpies for EB ethylation reaction. However, there are similar studies on different aromatic alkylation. For example, Bhandarkar et. al. [46] showed that the activation energy of toluene ethylation over ZSM-5 catalyst is 61.78 kJ/mole and the heat of adsorption of ethanol is 34.66 kJ/mole which is close to the results of this work. Also, a work presented by Sridevi. et al. [44] on the kinetics of benzene ethylation over $AlCl_3$-impregnated 13X catalyst, found that the activation energy for EB formation was 60.03 kJ/mole which is slightly higher than the value obtained from this study using mordenit catalyst (45.2 kJ/mole).

The estimated adsorption constants for ethylbenzene ethylation are reported in Table 4.9. One cans see that adsorption constant of ethanol is slightly higher compared to the adsorption constant of diethylbenzene over both catalyst samples. On the other hand, the estimated adsorption enthalpies reported in Table 4.8 shows that on both HZ-150 and MOR-180 catalysts, the enthalpies of adsorption of EtOH are lower than the enthalpies of adsorption of DEB. The model results address that EtOH and DEB both are adsorbed on the active sites. The estimated adsorption enthalpies and adsorption constants gave an indication for their comparable adsorption strength.

Finally, the estimated kinetic parameters for the fitted parameters substituted into the developed model equations and numerically solved using fourth order Runge-Kutta routine. The model predicted and experimental EB conversion and DEB yield are

compared in Figure 4.20. Both the predicted conversions and yield data fit the experimental data in an excellent manner.

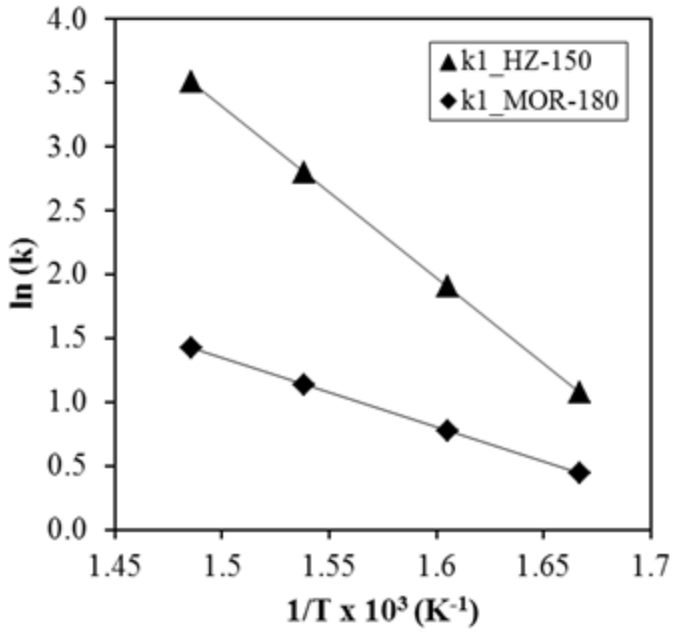

Figure 4.18. Arrhenius plot – ethylation reaction rate constant ln(k) vs 1/T data.

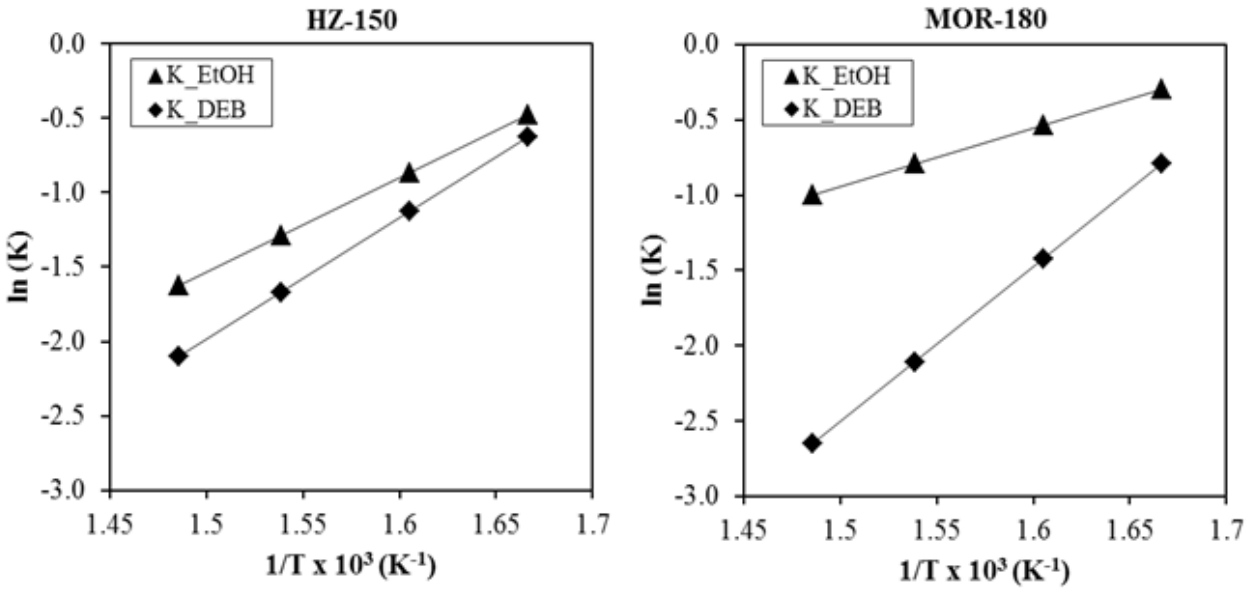

Figure 4.19. Van't Hoff plot – Equilibrium constants ln(K) vs 1/T data.

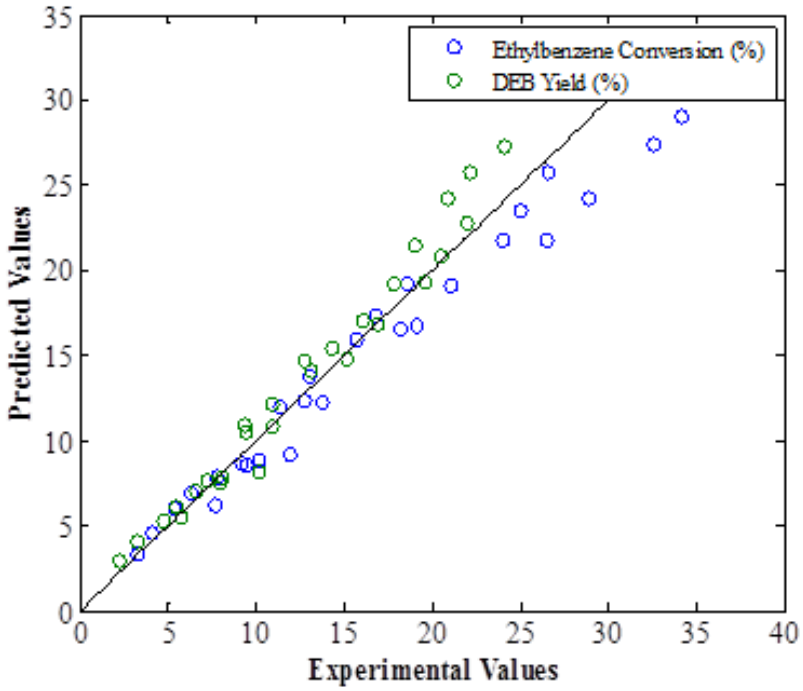

Figure 4.20. Reconciliation plot between model predictions and experimental data. Experimental data: data points, model prediction: continuous line.

CHAPTER 5

CONCLUSIONS

5.1 CONCLUSIONS

A novel fluidized bed process for the production of diethylbenzene through ethylbenzene ethylation and disproportionation over zeolite based catalysts was successfully investigated. The study was carried out using fluidizable catalysts based on ZSM-5 and mordenite based catalyst. Unlike previous studies which lay much emphasis on catalysis design, this work brings into consideration a new perspective which is aimed at improving the overall efficiency of the process by studying the effects of fluidization and the use of short contact times on ethylbenzene ethylation. As expected, fluidization led to a more uniform product distribution in comparison to fixed bed processes where temperature gradients in the reactor can negatively affect the product quality. It was also found that significant ethylbenzene conversion was achieved using short contact times (0-20 sec.) owing to fluidization.

5.1.1. Effect of zeolites acidity on ethylbenzene activity:

The physicochemical characterization of HZSM-5 catalysts with five different SiO_2/Al_2O_3 ratios, reaction and kinetics study of EB disproportionation and EB ethylation

with ethanol using these catalysts has been carried out. The following conclusions were drawn from the study:

i. The physicochemical characterizations results shows that the variation of SiO_2/Al_2O_3 ratios mainly affected the acidity of the catalysts while the specific surface area and the crystal structure and crystal sizes remain almost unchanged.

ii. Low temperature favors the EB ethylation reaction while higher temperature is favorable for both disproportionation and cracking reactions. In both the reactions, the EB conversion increases significantly with the increase of reaction temperature.

iii. In EB ethylation the DEB selectivity is almost the double of DEB selectivity in EB disproportionation while the benzene selectivity just opposite. The formation of benzene in ethylation is much lower.

iv. The amount of benzene in the reaction product increased as the temperature and reaction time were raised, showing that cracking reaction is favored at higher temperature and contact time.

v. The HZSM-5 catalyst with SiO_2/Al_2O_3= 80 seems to be the most effective giving superior activity and selectivity towards DEB.

vi. P-DEB selectivity is very high using HZ-280 catalyst, because of its low acidity lead to minimize the isomerization of p-DEB to m-DEB; however EB conversion and the products yield for this catalyst is comparable to the other catalysts in this study.

vii. Kinetic analysis of the reactions shows that during the EB disproportionation, the value of the activation energy for EB cracking is comparable to the activation

energy of EB disproportionation which is consistent to the high benzene selectivity in this route. On the other hand, during the EB ethylation with ethanol, a small amount of benzene was formed via the cracking of EB, which has been reflected by higher activation energy of the EB cracking reaction. The kinetics analysis also confirms that during EB ethylation the disproportionation of EB is negligible.

viii. In EB ethylation, the HZSM-5 catalyst with SiO_2/Al_2O_3= 80 requires lowest amount of activation energy to form p-DEB which was reflected in higher p-DEB yield of the catalyst.

ix. Although, the DEB yield of the SiO_2/Al_2O_3 = 80 catalyst is high, the p-DEB selectivity with such catalyst is comparable to the other catalysts studied in this study.

5.1.2 Effect of zeolites pore structure on ethylbenzene activity:

Phenomenological kinetics modeling of ethylbenzene alkylation with ethanol over ZSM-5 (medium pore zeolite) and mordenite (large pore zeolite) catalysts has been carried out. The following conclusions were drawn from the study:

i. Diethylbenzene is the main product during EB ethylation which is ethylated further to triethylbenzene over large pore zeolite indicates that large pore zeolite is more favorable for alkylation reactions than medium pore zeolite.

ii. DEB yield increase with increasing the reaction temperature reach to maximum point at 300^{o}C then start to decrease, indicate the increase of cracking and secondary alkylation reactions at high temperature.

iii. Large pore zeolite favors the formation of large molecules while the medium pore zeolite restricts there formation due to diffusional restriction.

iv. The kinetic analysis shows that EB ethylation reaction over both catalysts follows Langmuir-Hinshelwood mechanism where EB weakly adsorbed on the catalyst site compare to ethanol and DEB.

v. Large pore zeolite requires lowest amount of activation energy to form DEB compare to medium pore zeolite, which is reflect the ease of EB ethylation over large pore zeolite.

References

[1] H.G. Franck, J.W. Stadelhofer, Industrial Aromatic Chemistry, Springer-Verlag, Berlin-Heidelberg, 1988.

[2] S.M. Waziri, S. Al-Khattaf, Kinetics of ethylbenzene ethylation with ethanol over a ZSM-5-based catalyst in a riser simulator. Ind. Eng. Chem. Res. 48 (2009) 8341–8348.

[3] T-C. Tsai, S-B. Liu, I. Wang, Disproportionation and transalkylation of alkylbenzenes over zeolite catalysts, Appl. Catal. A: Gen. 181 (1999) 355–398.

[4] N. M. Tukur, S. Al-Khattaf, Comparative study between Ethylbenzene disproportionation reaction and its ethylation reaction with Ethanol over ZSM-5, Catal. Lett. 131 (2009) 225–233.

[5] S-H. Park, H-K. Rhee, Shape selective properties of MCM-22 catalysts for the disproportionation of ethylbenzene, Appl. Catal. A: Gen. 219 (2001) 99–105.

[6] K. Raj, J. Antony., M.S. Meenakshi, V.R. Vijayaraghavan, Ethylation and disproportionation of ethylbenzene over substituted AFI type molecular sieves, J. Mol. Catal. A: Chem. 270 (2007) 195–200.

[7] Y.S. Bhat, J. Das, A.B. Halgeri, Chemical Weekly 20 (1996) 163.

[8] Ullmann's Encyclopaedia of Industrial Chemistry, 1996. Volume A5, 5th Edition, VCH, 314-362.

[9] Dyer, A., 1988. An introduction to zeolite molecular sieves. Great Britain: John Wiley & Sins Ltd.

[10] MacQuarrie, D. J., 2000. Chemistry on the inside: green chemistry in mesoporous materials. Philosophical Transactions of the Royal Society A: Mathematical, Physical and Enginnering Sciences 358, 419-430.

[11] Perot, G., Guisnet, M., 1990. Advantages and disadvantages of zeolites as catalysts in organic chemistry. Journal of Molecular Catalysis 61, 173-196.

[12] Jao, R. M., Leu, L. J., Chang, J. R., 1996. Effects of catalyst preparation and pre-treatment on light naphtha isomerisation over mordenite-supported Pt catalysts: Optimal reduction temperature for pure feed and foe sulphur-containing feed. Applied Catalysis A: General 135, 301-316.

[13] Reschetilowski, W., Mroczek, U., Steinberg, K. H.,1991. Influence of platinum dispersion on the ethane aromatisation on Pt/H-ZSM-5 zeolite. Applied Catalysis 78, 257-264.

[14] Smirniotis, P. G., Ruchenstein, E., 1993. Comparison between zeolite β and γ-Al2O3 supported Pt for reforming reactions. Journal of Catalysis 140, 526-542.

[15] Armaroli, T., Simon, L. J., Digne, M., Montanari, T., Bevilacqua, M., Valtchev, V., Patarin, J., Busca, G., 2006. Effects of crystal size and Si/Al ratio on the surface properties of H-ZSM-5 zeolites. Applied Catalysis A: General 306, 78-84.

[16] Dimitrova, R., Gunduz, G., Spassova, M., 2006. A comparative study on the structural and catalytic properties of zeolites type ZSM-5, mordenite, Beta and MCM-41. Journal of Molecular Catalysis 243, 17-23.

[17] Trombetta, M., Alejandre, A. G., Solis, J. R., Busca, G., 2000. An FT-IR study of the reactivity of hydrocarbons on the acid sites of HZSM5 zeolite. Applied Catalysis A: General 198, 81-93.

[18] Wanger P, Nakagawa Y ,Lee GS, Davis ME, Elomari S, Medurd RC, Zones SI (2000) J Am Chem Soc 122:263.

[19] Cejka, J.; Wichterlova, B., Acid-catalyzed synthesis of mono-and dialkylbenzenes over zeolites: Active sites, zeolite Topology and reaction mechanisms. Catal. Rev. 2002, 44, 375-421.

[20] Zhu, Z.; Chen, Q.; Xie, Z.; Yang, W.; Kong, D.; Li. C. Shape-selective disproportionation of ethylbenzene to para-diethylbenzene over ZSM-5 modified by chemical liquid deposition and MgO. J. Mol. Catal. A: Chem. 2006, 248, 152–158.

[21] Wichterlovfi, B; Cejka, J. A comparison of the ethylation of ethylbenzene and toluene on acid, cationic and silylated ZSM-5 zeolites. Catalysis Letters 1992, 16, 421-429.

[22] Z. Zhirong, C. Qingling, X. Zaiku, Y. Weimin, K. Dejin, Li, Can., Shape-selective disproportionation of ethylbenzene to para-diethylbenzene over ZSM-5 modified by chemical liquid deposition and MgO, J. Mol. Catal. A: Chem. 248 (2006), 152–158.

[23] G.D. Yadav, P.K. Goel, A new efficient catalyst UDCaT-1 for the alkylation of ethylbenzene with ethanol to diethylbenzene, Clean Tech. Env. Pol. 4 (2002), 165–170.

[24] X. Guan, N. Li, G. Wu, J. Chen, F. Zhang, N. Guan, Para-selectivity of modified HZSM-5 zeolites by nitridation for ethylation of ethylbenzene with ethanol, J. Mol. Catal. A: Chem. 48 (2006), 220–225.

[25] J. Cejka, B. Wichterlova, Acid-catalyzed synthesis of mono- and dialkyl benzenes over zeolites: Active sites, zeolite topology and reaction mechanisms, Catal. Rev. 44 (2002) 375.

[26] I.V. Mishin, H.K. Beyer, H.G. Karge, Activity and selectivity of high-silica mordenites in the disproportionation of ethylbenzene, Appl. Catal. A: Gen. 180 (1999) 207–216.

[27] W-H. Chen, T-C. Tsai, S-J. Jong, Q. Zhaoa, C-T.Tsai, I. Wang, H-K. Lee, S-B. Liu, Effects of surface modification on coking, deactivation and para-selectivity of H-ZSM-5 zeolites during ethylbenzene disproportionation, J. Mol. Catal. A: Chem. 181 (2002), 41–55.

[28] Y. Sugi, Y. Kubota, K. Komura, N. Sugiyama, M. Hayashi, J-H. Kim, H-ZSM-5 modified with lanthanum and cerium oxides in shape-selective ethylation of ethylbenzene. The deactivation of external acid sites and the control of pore entrance, Stud. Surf. Sci. Catal. 158 (2005), 1279–1286.

[29] R.B. Weber, J.C.Q. Fletcher, K.P. Möller, C.T. O'Connor, The characterization and elimination of the external acidity of ZSM-5, Microp. Mesop. Mater. 7 (1996) 15-25.

[30] H.P. Röger, M. Krämer, K.P. Möller, C.T. O'Connor, Effects of in-situ chemical vapour deposition using tetraethoxysilane on the catalytic and sorption properties of ZSM-5, Microp. Mesop. Mater. 21 (1998) 607-614.

[31] S. Al-Khattaf, N. Tukur, S. Rabiu, Ethylbenzene Transformation over a ZSM-5-Based Catalyst in a Riser Simulator, Ind. Eng. Chem. Res. 48 (2009) 2836–2843.

[32] Maxwell, I. E.; Stork, W. H. J. Chapter 17 Hydrocarbon processing with zeolites. *Studies in Surface Science and Catalysis* **2001**, 137, 747-819.

[33] Odedairo, T.; Al-Khattaf, S. Comparative study of zeolite catalyzed alkylation of benzene with alcohols of different chain length: H-ZSM-5 versus mordenite. *Catalysis Today* **2013**, 204, 73– 84.

[34] Waziri, S. M.; Aitani, A. M.; Al-Khattaf, S. Transformation of Toluene and 1,2,4-Trimethylbenzene over ZSM-5 and Mordenite Catalysts: A Comprehensive Kinetic Model with Reversibility. *Ind. Eng. Chem. Res.* **2010,** *49*, 6376–6387.

[35] Arsenova-Hartel, N.; Bludau, H.; Haag1, W. O.; Karge, H. G. Influence of the zeolite pore structure on the kinetics of the disproportionation of ethylbenzene. *Microporous and Mesoporous Materials* **2000**, 35-36, 113-119.

[36] Arsenova, N.; Haag, W. O.; Karge, H.G. Kinetics study of ethylbenzene disproportionation with medium and large pore zeolites. *Stud. Surf. Sci. Catal*. **1997**, 105, 1293–1300.

[37] Perego, C., Ingallina, P., 2002. Recent advances inthe industrial alkylation of aromatics: new catalysts and new processes. Catalysis Today 73, 3-22.

[38] Moreau, F., Gnep, N. S., Lacombe, S., Merlen, E., Guisnet, M., 2002. Ethylbenzene transformation on bifunctional Pt/Al_2O_3-NaHMOR catalysts. Influence of Na exchange 221 on their activity and selectivity in ethylbenzene isomerisation. Applied Catalysis A: General 230, 253-262.

[39] Caeiro, G., Carvalho, R. H., Wang, X., Lemos, M.A.N.D.A., Lemos, F., Guisnet, M., Ramoa Ribeiro, F., 2006. Activation of C2-C4alkanes over acid and

bifunctional zeolite catalysts. Journal of Molecular Catalysis A: Chemical 255, 131-158.

[40] Ivanova, I. I., Nesterenko, N. S., Fernandez, C., 2006. In situ MAS NMR studies of alkylaromatics transformations over acidic zeolites. Catalysis Today 113, 115-125.

[41] Santilli, D. S., 1986. The mechanism of aromatic transalkylation in ZSM-5. Journal of Catalysis 99, 327-334.

[42] Tsai, T., Wang, I., 1992. Disproportion mechanism study of probing by n-propylbenzene. Journal of Catalysis 133, 136-145.

[43] N. Arsonova, H. Bludau, R. Schumacher, W.O. Haag, H.G. Karge, E. Brunner, U. Wild, Catalytic and sorption studies related to the para selectivity in the ethylbenzene disproportionation over H-ZSM-5 catalysts, J. Catal. 191 (2000) 326–331.

[44] Sridevi, U.; Rao, B. K. B.; Pradhan, N. C. Kinetics of alkylation of benzene with ethanol on $AlCl_3$-impregnated 13X zeolites. *Chem. Eng. J.* **2001**, 83, 185–189.

[45] Mantha, R.; Bhatia, S.; Rao, M. S. Kinetics of Deactivation of Methylation of Toluene over H-ZSM-5 and Hydrogen Mordenite Catalysts. *Ind. Eng. Chem. Res*. **1991**, 30, 281-286.

[46] Bhandarkar, V.; Bhatia, S. Selective formation of ethyltoluene by alkylation of toluene with ethanol over modified HZSM-5 zeolites. *Zeolites* **1994**, 14, 439-449.

[47] Lee, B. J.; Wang, I. Kinetic Analysis of Ethylation of Toluene on HZSM-5. *Ind. Eng. Chem.* **1985**, 24, 201-205.

[48] Corma, A.; Martinez-Soria, V.; Schnoeveld, E.; Alkylation of Benzene with Short-Chain Olefins over MCM-22 Zeolite: Catalytic Behaviour and Kinetic Mechanism. *Journal of Catalysis* **2000**, 192, 163–173.

[49] Smirniotis, P. G.; Ruckenstein, E. Alkylation of Benzene or Toluene with MeOH or C_2H_4 over ZSM-5 or β Zeolite: Effect of the Zeolite Pore Openings and of the Hydrocarbons Involved on the Mechanism of Alkylation. *Ind. Eng. Chem. Res.* **1996**, 34, 1517-1528.

[50] Schumacher R., Karge, H. G., 1999. Sorption kinetics study of the diethylbenzene isomers in MFI-type zeolites. Microporous and Mesoporous Materials 30, 307-314.

[51] Kaeding, W. W., 1985. Shape-selective reactions with zeolite catalysts: V. Alkylation or disproportionation of ethylbenzene to produce p-diethylbenzene. Journal of Catalysis 95, 512-519.

[52] de Lasa, H. I. Riser simulator for catalytic cracking studies. U.S. Patent 5, 1992, 102, 628.

[53] J. Pruski, A. Pekediz, H. de Lasa, Catalytic cracking of hydrocarbons in a novel riser simulator. Lump adsorption parameters under reaction conditions, Chem. Engng. Sci. 51 (1996) 1799-1806.

[54] D.W. Kraemer, U. Sedran, H.I. de Lasa, Catalytic cracking kinetics in a novel riser simulator, Chem. Engng. Sci. 45 (1990) 2447–2452.

[55] H-K. Min, S.B. Hong, Mechanistic investigations of ethylbenzene disproportionation over Medium-Pore Zeolites with Different Framework Topologies, J. Phy, Chem. C 115 (2011), 16124–16133.

[56] H.G. Karge, J. Ladebeck, Z. Sarbak, K. Hatada, Conversion of alkylbenzenes over zeolite catalysts. I. Dealkylation and disproportionation of ethylbenzene over mordenites, Zeolites, 2 (2) (1982), 94-102.

[57] H.G. Karge, K. Hatada, Y. Zhang, R, Fiedorow, Conversion of alkylbenzenes over zeolite catalysts II. Disproportionation of ethylbenzene over faujasite-type zeolites. Zeolites, 3 (1) (1983), 13-21.

[58] B. Rajesh, M., Palanichamy, V. Kazansky, V. Murugesan, Ethylation of ethylbenzene with ethanol over substituted medium pore aluminophosphate-based molecular sieves, J. Mol. Catal A: Chem. 187 (2002) 259–267.

[59] S. Al-Khattaf, Catalytic transformation of ethylbenzene over Y-zeolite-based catalysts, Energy Fuels 22 (2008) 3612–3619.

[60] A.B. Halgeri, D. Jagannath, Recent advances in selectivation of zeolites for *para*-disubstituted aromatics, Catal. Today 73 (2002), 65–73.

[61] Sharnappa, N.; Pai, S.; Bokade, V. V. Selective alkylation and disproportionation of ethylbenzene in the presence of other aromatics. *J. Mol. Catal. A: Chem.* 2004, 217, 185–191.

[62] N. Sharnappa, S. Pai, V.V. Bokade, Disproportionation of ethylbenzene in the presence of C_8 aromatics, J. Natural Gas Chem. 18 (2009) 369–374.

[63] C.M. Zhang, Z. Xu, K.S. Wan, Q. Liu, Synthesis, characterization and catalytic properties of nitrogen-incorporated ZSM-5 molecular sieves with bimodal pores, Appl. Catal. A 258 (2004) 55-61.

[64] J.-H. Kim, S. Namba, T. Yashima, Para-selectivity of metallosilicates with MFI zeolite structure, Zeolites 11 (1991) 59-63.

[65] Mentzel, U. V.; Højholt, K. T.; Holma, M. S.; Fehrmann, R.; Beato, P. Conversion of methanol to hydrocarbons over conventional and mesoporous H-ZSM-5 and H-Ga-MFI: Major differences in deactivation behavior. *App. Catal. A* **2012**, 417–418, 290– 297.

[66] K. Tocha, J.W. Thybauta,∗, B.D. Vandegehuchtea, C.S.L. Narasimhanb, L. Domokosb, G.B. Marin, A Single-Event MicroKinetic model for "ethylbenzene dealkylation/xylene isomerization" on Pt/H-ZSM-5 zeolite catalyst, Applied Catalysis A: General 425–426 (2012) 130–144.

[67] Sotelo, J. L.; Uguina, M. A.; Valverde, J. L.; Serrano, D. P. Kinetics of Toluene Alkylation with Methanol over Mg-Modified ZSM-5. *Ind. Eng. Chem. Res*. **1993**, 32, 2548-2554.

[68] Schwaab, M.; Lemos, L. P.; Pinto, J. C. Optimum reference temperature for reparameterization of the Arrhenius equation. Part 2: Problems involving multiple reparameterizations. *Chem, Eng. Sci*. **2008**, 63, 2895-2906.

[69] Smith, J. M.; Van Ness, H. C.; Abbott, M. M. Introduction to Chemical Engineering Thermodynamics. Mcgraw-Hill: New York, 2001;

[70] Hossain, M. M.; Atanda, L.; Al-Yassir, N.; Al-Khattaf, S. Kinetics Modeling of Ethylbenzene Dehydrogenation to Styrene over a Mesoporous Alumina Supported Iron Catalyst. *Chem. Eng. J*. **2012**, 207–208, 308–321.

[71] Al-Khattaf, S.; Atias, J.A.; Jarosch, K.; de Lasa, H. Diffusion and catalytic cracking of 1,3,5 tri-iso-propyl-benzene in FCC catalysts. *Chem, Eng. Sci*. **2002**, 57, 4909-4920.

[72] Barman, S.; Maity, S. K.; Pradhan, N. C. Alkylation of toluene with isopropyl alcohol catalyzed by Ce-exchanged NaX zeolite. *Chem. Eng. J*. **2005**, 114, 39–45.

Vitae

Name	: Mogahid Saifeldin Idris Osman
Nationality	: Sudanese
Date of Birth	:5/13/1988
Email	: mogahidsaif@gmail.cm
Address	: King Fahd University of Petroleum & Minerals, Dhahran
Academic Background	: B.Sc. Chemical Engineering – University of Khartoum

Research Outcomes

Journal Publications:

- **M. Osman**, L. Atanda, M. M. Hossain, S. Al-Khattaf, Kinetics modeling of disproportionation and ethylation of ethylbenzene over HZSM-5: Effects of SiO_2/Al_2O_3 ratio, ***Chemical Engineering Journal***, 222 (2013) 498-511.

- **M. Osman**, M. M. Hossain, S. Al-Khattaf, Kinetics study of ethylbenzene alkylation with ethanol over medium and large pore zeolites. ***Industrial and Engineering Chemistry Research Journal***, 52 (2013) 13613-13621.

Conferences Contribution:

- **M. Osman**, M. M. Hossain, S. Al-Khattaf. (2013), Effects of Zeolites Structure and Acidity on Ethylbenzene Disproportionation and Ethylation. The 3rd KACST-Oxford Petrochemical Forum, August 12^{th}-15^{th}, 2013, Oxford, UK.

- **M. Osman**, M. M. Hossain, S. Al-Khattaf. (2013), Ethylation and disproportionation of ethylbenzene to diethylbenzene over HZSM-5 catalysts: Effects of SiO_2/Al_2O_3 ratio, 4^{th} Scientific Conference for Students of Higher Education in Saudi Arabia, Apr 29^{th} – May 2^{nd}, Mecca, Saudi Arabia.